

# Submarine landslides: processes, triggers and hazard prediction

BY D. G. MASSON<sup>1,\*</sup>, C. B. HARBITZ<sup>2</sup>, R. B. WYNN<sup>1</sup>, G. PEDERSEN<sup>3</sup>  
AND F. LØVHOLT<sup>2</sup>

<sup>1</sup>*National Oceanography Centre, Southampton SO14 3ZH, UK*

<sup>2</sup>*Norwegian Geotechnical Institute, International Centre for Geohazards,  
PO Box 3930 Ullevaal Stadion, 0806 Oslo, Norway*

<sup>3</sup>*Department of Mathematics, University of Oslo, International Centre for  
Geohazards, PO Box 1053 Blindern, 0316 Oslo, Norway*

Huge landslides, mobilizing hundreds to thousands of km<sup>3</sup> of sediment and rock are ubiquitous in submarine settings ranging from the steepest volcanic island slopes to the gentlest muddy slopes of submarine deltas. Here, we summarize current knowledge of such landslides and the problems of assessing their hazard potential. The major hazards related to submarine landslides include destruction of seabed infrastructure, collapse of coastal areas into the sea and landslide-generated tsunamis. Most submarine slopes are inherently stable. Elevated pore pressures (leading to decreased frictional resistance to sliding) and specific weak layers within stratified sequences appear to be the key factors influencing landslide occurrence. Elevated pore pressures can result from normal depositional processes or from transient processes such as earthquake shaking; historical evidence suggests that the majority of large submarine landslides are triggered by earthquakes. Because of their tsunamigenic potential, ocean-island flank collapses and rockslides in fjords have been identified as the most dangerous of all landslide related hazards. Published models of ocean-island landslides mainly examine ‘worst-case scenarios’ that have a low probability of occurrence. Areas prone to submarine landsliding are relatively easy to identify, but we are still some way from being able to forecast individual events with precision. Monitoring of critical areas where landslides might be imminent and modelling landslide consequences so that appropriate mitigation strategies can be developed would appear to be areas where advances on current practice are possible.

**Keywords:** submarine landslides; landslide processes; landslide causes; tsunamis; landslide hazards; hazard prediction

## 1. Introduction

Submarine landslides are one of the main agents through which sediments are transferred across the continental slope to the deep ocean. Sediments derived from land (mainly carried by rivers) and from the continental shelf (e.g. through

\* Author for correspondence (dgm@noc.soton.ac.uk).

One contribution of 20 to a Discussion Meeting Issue ‘Extreme natural hazards’.

erosion and transport by ocean currents and storms) are, in the first instance, often deposited on the upper continental slope where they may be interbedded with pelagic sediments settling from the water column. However, these deposits often equate only to temporary storage, as instability in the slope deposits leads to periodic slope failure, landsliding and onward downslope transport. The human consequences can be severe and include destruction of seabed infrastructure (e.g. telecommunications cables), subsidence of coastal areas and generation of damaging tsunamis. In this latter respect, flank collapses on oceanic islands, which consist largely of rock (rather than sediment) and have both subaerial and submarine components, pose a particular threat. The aim of this paper is to summarize key aspects of submarine landslides, especially where these relate to their hazard potential, and assess our ability (or lack of ability) to predict where and when future submarine landslides will occur.

Landslide terminology is beyond the remit of this paper, but as noted by several authors (Hampton *et al.* 1996; Mulder & Alexander 2001; Canals *et al.* 2004) the reader should be aware of the complexity of landslide nomenclature and the frequent imprecise use of landslide terminology, especially in the submarine environment where information on landslide processes is often limited. In this paper, ‘landslide’ is used as a generic term encompassing all forms of slope failure, irrespective of process. Other terms used in this paper, including ‘slide’, ‘debris flow’, ‘debris avalanche’ and ‘turbidity current’, each imply a particular process as defined below:

Slide: movement of a coherent mass of sediment bounded by distinct failure planes.

Debris flow: laminar, cohesive flow of clasts in a fine-grained matrix (e.g. wet concrete).

Debris avalanche: rapid flow of cohesionless rock fragments with energy dissipation by grain contact.

Turbidity current: gravity flow in which sediment grains are maintained in suspension by fluid turbulence.

## 2. Occurrence, distribution and scale of submarine landslides

Landslides are widespread on submarine slopes, particularly in areas where fine-grained sediments predominate (figure 1). In the North Atlantic, this corresponds mainly to areas at high and low latitudes (Weaver *et al.* 2000) and appears to correlate with the weathering style of rocks on land. In general, glacial action at high latitudes and chemical weathering processes at low latitudes produce fine-grained sediments that form thick accumulations on the continental slope and appear to favour landslide formation. Between these zones, at mid-latitudes, fluvial weathering and sediment transport produces greater quantities of coarser grained sediment. This sediment is often transported directly to the deep ocean basins by turbidity currents, which pass through submarine canyons and bypass the slope. Although small landslides frequently occur on canyon margins, adjacent slopes are relatively starved of sediment and appear less likely to be affected by landslides. The submarine deltas and fans of large rivers are also subject to widespread landsliding, related to the rapid accumulation of fine-grained sediments on the continental slope (e.g. Mississippi

Fan; Prior & Coleman 1982). Landslides in fjords (Jorstad 1968) and on the flanks of oceanic islands pose particular hazards to humans. In fjord environments, landslides are frequently associated with ‘quick clay’, a particularly unstable sediment created when marine clays are uplifted above sea level (usually by glacial rebound) and leached by fresh water (Locat *et al.* 2003). Failure of submarine deltas formed where rivers discharge sediment onto the steep submarine walls of fjords is also common (Prior *et al.* 1982; Kulikov *et al.* 1996). Landslides on ocean-island flanks have been cited as posing a tsunami threat on a trans-oceanic scale (Ward & Day 2001), potentially comparable in magnitude to or even larger than the 2004 Indian Ocean tsunami (Lay *et al.* 2005). While this extreme scenario can be questioned (Mader 2001; Wynn & Masson 2003), there is little doubt that the threat posed by ocean-island flank landslides is both real and significant.

Hühnerbach *et al.* (2004) have recently documented the distribution of landslides on North Atlantic margins. Although the quality and completeness of many of the published descriptions of submarine landslides were limited, these authors were able to conclude that:

- (i) The occurrence of landslides is not greatly influenced by slope gradients, except at the shallowest gradients where relatively few landslides occur (figure 2).
- (ii) There is a suggestion that the largest landslides on the continental slope occur on the lowest slopes, often as low as  $1^\circ$ .
- (iii) The greatest number of landslide headwalls occur on the mid-slope, with a peak at 1000–1300 m waterdepth, rather than at the shelf edge or on the upper slope as might be expected (figure 2).

The largest submarine landslides can involve many thousand  $\text{km}^3$  of material, two to three orders of magnitude larger than any terrestrial landslide (table 1; Hampton *et al.* 1996). For example, the Storegga slide involved some  $3000 \text{ km}^3$  of sediment, affected  $95\,000 \text{ km}^2$  of the Norwegian slope and basin and had a run-out distance of around 800 km (Hafidason *et al.* 2004). To put this into perspective, the area is about 20% bigger than Scotland and the run-out is close to the length of mainland Britain.

The largest landslides occur mainly in two settings, on open continental margins and on oceanic island flanks. This appears to be a function of specific aspects of the geology and morphology of these areas. Continental margin slopes that are subject to large-scale failures are typically of low gradient (from less than  $1^\circ$  to  $5^\circ$ ) with gentle topography; however, the ‘drop’ from shelf edge to basin floor can be up to 5 km over distances of a few hundred kilometres. Parallel-bedded sediment sequences with little variability over large areas characterize their sub-surface structure, with the result that, should the conditions for slope failure occur, they can simultaneously affect large areas.

When measured from the top of the highest volcano to the bottom of the adjacent ocean basin, ocean islands such as Hawaii and the Canary islands have the greatest relief of any topographic feature on Earth. The island slopes can be very steep (e.g. on Tenerife in the Canary islands the average slope from the top of Teide volcano to the coast is  $15^\circ$ ) and volcanic processes tend to build, load and steepen these slopes with time. Despite this, not all these slopes are unstable,

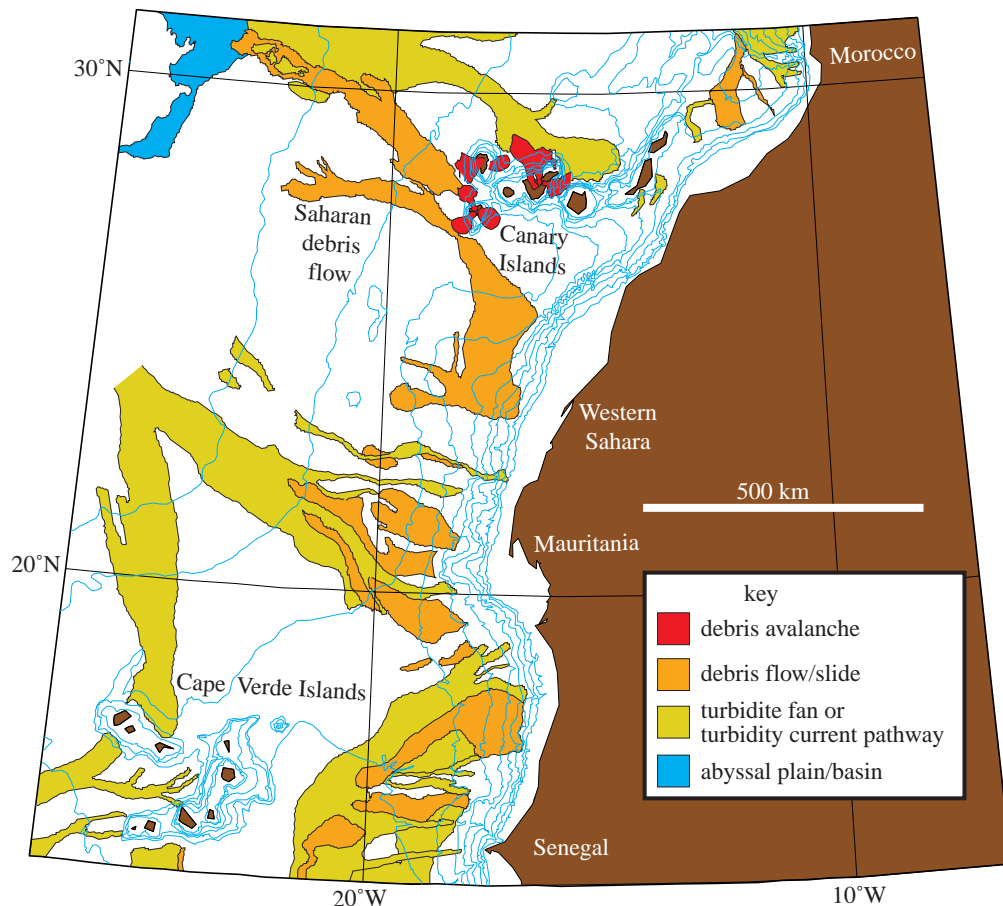


Figure 1. Distribution of landslides and landslide deposits on the seafloor of the NW African margin. The map shows the degree to which this margin has been impacted by landslides in the recent geological past. When extrapolated into three dimensions the importance of landslides in the margin building process is obvious.

with landslide occurrence apparently closely controlled by geology, particularly the trends of dyke intrusion (rift zones) on the islands (Moore *et al.* 1989; Carracedo 1996; Masson *et al.* 2002).

However, as discussed in the following section, a landslide's size is not necessarily proportional to the hazard it poses. In particular, continental margin landslides that occur on very low slopes, far from land, may form relatively slowly by retrogressive processes, similar to quick clay flows on land (Bentley & Smalley 1984). Many such landslides appear to have limited tsunamigenic potential, although they may still pose a threat to cables or other seabed installations.

### 3. Submarine landslides and hazards

The hazard posed by submarine landslides will vary according to landslide scale, location, type and process. Even small submarine landslides can be dangerous when they occur in coastal areas. The 1996 Finneidfjord slide, in northern

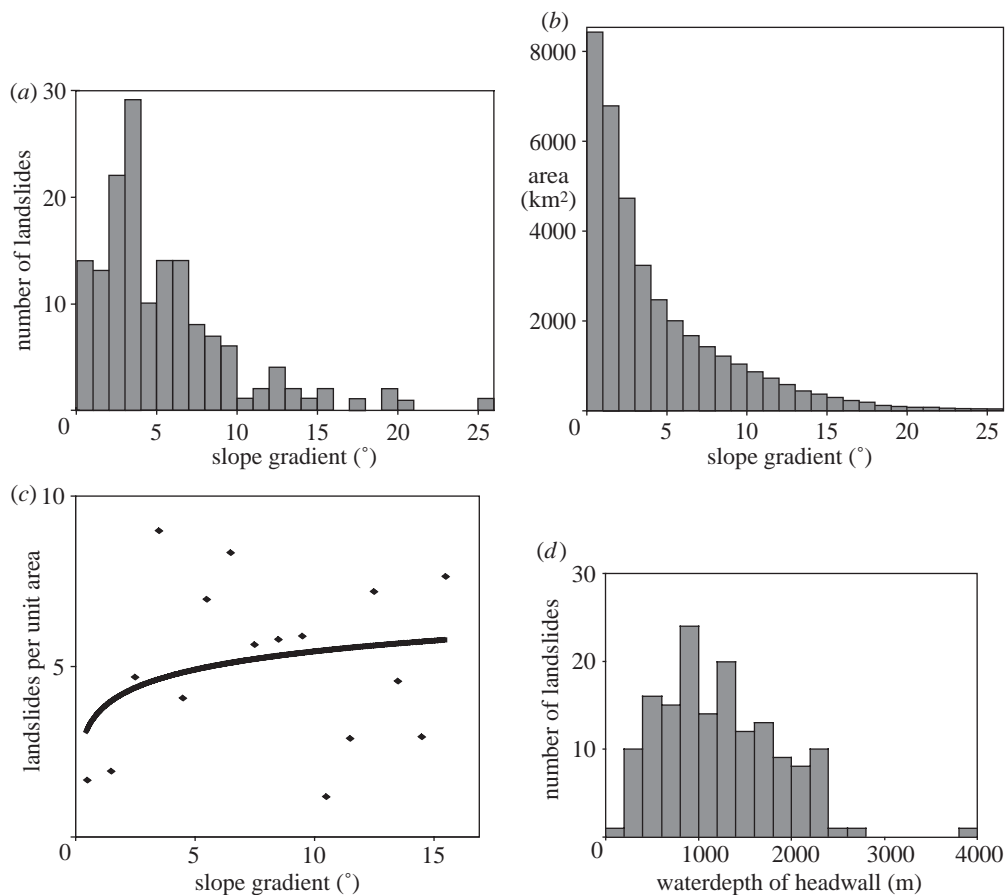


Figure 2. (a) Numbers of landslides on the eastern continental slope of North America between 30 and 45°N, plotted against slope in the landslide headwall area. (b) Distribution of slope gradients between 36 and 37°N and between 200 and 3000 m water depth on the eastern North American slope (extracted from multibeam data gridded at 100 m). Comparison of the histogram shapes in (a) and (b) suggests that landslide occurrence is largely independent of slope angle at gradients more than 3°, but that landslides are relatively rarer on lower slope gradients. A plot of landslide occurrence per unit area against slope gradient (c) gives some support to the qualitative comparison of (a) and (b) based on histogram shape, although the correlation in (c) is weakened by the scatter of data points which is mainly due to the low numbers of observed landslides. (d) Number of landslides plotted against water depth in the headwall region, indicating that most landslides are initiated in mid-slope. Similar distributions of landslides are seen in the eastern Atlantic confirming the robustness of the interpretations based on (a)–(d) above (Hühnerbach *et al.* 2004).

Norway, mobilized only 0.001 km<sup>3</sup> of sediment and little of this material travelled more than a few hundred metres from source, but four people were killed when a house and car were carried away (Longva *et al.* 2003). The 1979 Nice airport slide also cut back onto land, killing several men working on the airport extension (Assier-Rzadkiewicz *et al.* 2000). However, the effects of this landslide were felt at least 100 km offshore, where a turbidity current generated by the landslide broke submarine telephone cables. A local tsunami, which resulted in the death of one person, was also observed. The 1929 Grand Banks

Table 1. Examples of submarine landslides illustrating the range of size, the slopes on which they occur and the materials involved.

name (location)	failure type	sediment type	water depth (m)	area (km <sup>2</sup> )	length (km)	thickness of deposit (m)	volume (km <sup>3</sup> )	slope (°)	reference
Nuuanu slide (Hawaii)	debris avalanche	volcanic rock	0–4600	23 000	230	up to 2000	5000	?5–0	Moore <i>et al.</i> (1989)
El Golfo avalanche (Canaries)	debris avalanche	volcanic rock, volcanoclastic and pelagic sediment	1000 m above sea level to 3900 m below	1500	65	up to 200	150–180	10–1	Masson (1996)
Storegga slide/debris flow	slide/debris flow	glacigenic mud, interglacial oozes	200–3800	95 000	810	up to 430	2400–3200	1.4–0.05	Haffidason <i>et al.</i> (2004)
Saharan slide	slide/debris flow	volcanoclastic and pelagic sediment	1700–4800	48 000	700	5–40	600	1.6° to 0.05°	Gee <i>et al.</i> (1999)
Canary debris flow	slide/debris flow	volcanoclastic and pelagic sediment	4000–5400	40 000	600	up to 20	400	1–0	Masson <i>et al.</i> (1998)
f turbidite (Madeira Abyssal Plain)	turbidity current	pelagic sediment	?–5400	> 60 000	1000+	up to 5	190	< 2–0	Rothwell <i>et al.</i> (1992)
1929 Grand Banks turbidite	turbidity current	mixed glaci-genic sediment	600–6000	160 000	1000	? up to 3	200	? to 0.01	Fine <i>et al.</i> (2005), Piper <i>et al.</i> (1999)
Afen slide (Faroe-Shetland Channel)	debris flow	glaciomarine mud	830–1120	38	12	up to 8	0.14	2.5–0.7	Masson (2001), Wilson <i>et al.</i> (2004)

earthquake resulted in submarine landslides, a turbidity current, and a tsunami that caused significant casualties (Heezen & Ewing 1952; Piper *et al.* 1999; Fine *et al.* 2005). This is one of the best-known submarine landslides because the resultant turbidity current broke several submarine cables sequentially downslope, allowing the speed of such a current (up to  $30 \text{ m s}^{-1}$ ) to be measured for the first time. It also illustrates one of the main difficulties in submarine geohazard study—when a coupled earthquake/landslide generates a tsunami, which of the two hazards produces the tsunami or could their effects even be combined (Fryer *et al.* 2004; Fine *et al.* 2005)? The latter has been suggested for the 1998 tsunami that struck Papua New Guinea (PNG), killing over 2000 people (Satake & Tanioka 2003). However, there is now considerable evidence that many ‘unusual’ tsunamis, particularly those with high near-field run-ups that decay rapidly away from source, are directly caused by landslides (Bardet *et al.* 2003; Okal & Synolakis 2004). Rotational slides (often referred to as slumps), where a thick slide block with a steep headwall can move rapidly downward, may be particularly effective in generating tsunamis, even when the lateral distance moved is small and little effect is seen on the seafloor downslope of the immediate landslide site. The PNG tsunami is most likely to have been generated in this way (Matsumoto & Tappin 2003; Sweet & Silver 2003).

Finally, it should not be forgotten that an increasing proportion of the world’s oil and gas is now recovered from deep-water areas offshore, where slope instability can be a major geohazard. The juxtaposition of the Ormen Lange gas field, which is set to supply some 20% of UK natural gas requirements in future years, and the Storegga slide, brings this sharply into focus.

#### 4. Causes of landslides

Many factors have been suggested as probable or possible contributors to the initiation of submarine landslides (table 2). These vary from sudden impacts operating on timescales of minutes (e.g. shaking due to earthquakes) to geological processes operating on timescales of tens to hundreds of thousands of years (e.g. climate change; Weaver & Kuijpers 1983). Broadly, they can be divided into two types, those related to the geological characteristics of the landslide material (e.g. overpressure due to rapid deposition or the presence of a weak layer) and those driven by transient external events (e.g. earthquakes or climate change). In some cases, the relationship between a landslide and its cause is very obvious and direct (e.g. failure of an oversteepened slope). In others this relationship may not be obvious at all, especially where the link is indirect and involves some intermediate process. A good example of this is found on the Norwegian continental slope where the locations of landslides, such as the Storegga and Traenadjupet slides, can be related to the occurrence of specific geological horizons that act as weak layers (Laberg *et al.* 2003; Kvalstad *et al.* 2005). The distribution of these weak layers, however, is controlled by regional changes in sedimentation style, which, on an even broader scale, are driven by climate change between glacial and interglacial conditions (Bryn *et al.* 2005). On top of all of this, it has been calculated that an earthquake was still required to ultimately trigger these landslides (Bryn *et al.* 2005; Kvalstad *et al.* 2005)!

Table 2. Factors contributing to the initiation of submarine landslides. (Note that more than one factor may contribute to a single landslide event.)

historically documented	examples	references
earthquakes	Grand Banks	Fine <i>et al.</i> (2005)
hurricanes or cyclic loading	Mississippi delta	Prior & Coleman (1982)
loading or oversteepening of slopes	Nice, Canary islands	Assier-Rzadkiewicz <i>et al.</i> (2000)
underconsolidation (overpressure)	Mississippi delta	Prior & Coleman (1982)
rainfall (where landslides have a subaerial extension)	Norway, Hawaii	Longva <i>et al.</i> (1996)
slope parallel weak layers in bedded sequences	east coast US, Storegga, west Africa	O'Leary (1991), Haffidason <i>et al.</i> (2003), Bryn <i>et al.</i> (2005)
suggested (but less well documented)		
gas hydrate dissociation	east coast US, Storegga	Sultan <i>et al.</i> (2003)
sea-level change	Madeira Abyssal Plain	Weaver & Kuijpers (1983)
volcanic activity	Hawaii, Canaries	Moore <i>et al.</i> (1989), Masson <i>et al.</i> (2002)

The above example shows that many if not all landslides result from the coming together of more than one of the factors given in table 2. Most continental slope sediments, for example, are stable under all but the most extreme earthquake shaking, unless other factors, such as overpressured layers or sensitive sediments are present (Roberts & Cramp 1996; Kvalstad *et al.* 2005). Many large historical landslides, recognized because they broke telephone cables or caused collapse of river deltas in fjords or tsunamis, have coincided with earthquakes (Tappin *et al.* 2001; Fryer *et al.* 2004; Fine *et al.* 2005). This presumably reflects the long term persistence of 'geological' factors compared to the transient nature of earthquake shaking, such that the short-lived transient event is the final push which tips the balance between a stable slope and a landslide.

Human activities can also contribute to submarine landslide triggering. Although landslides generated in this way are usually small, they can often be very dangerous because they extend upslope onto land and can affect inhabited areas. Examples include the 1996 Finneidfjord landslide, where it has been hypothesized that the trigger was heavy rainfall combined with rock blasting (Longva *et al.* 1996), and the 1979 Nice Airport landslide, where loading of the upper slope during construction work at the airport probably contributed (Assier-Rzadkiewicz *et al.* 2000). In other areas where submarine landslides have directly affected human-made structures, such as where buildings on deltas have been submerged or offshore oil installations destroyed by landslides, it is often impossible to determine (and sometimes unlikely) that human activities triggered the landslides. However, even if human activity is not to blame for triggering such landslides, building in these areas has undoubtedly contributed to the landslide consequences.

The concept that 'weak layers' oriented parallel to sedimentary bedding might control the location of many continental slope landslides is not new (see O'Leary (1991) and references therein). However, it required the advent of modern seafloor survey technology, such as swath bathymetric mapping and 3D seismic

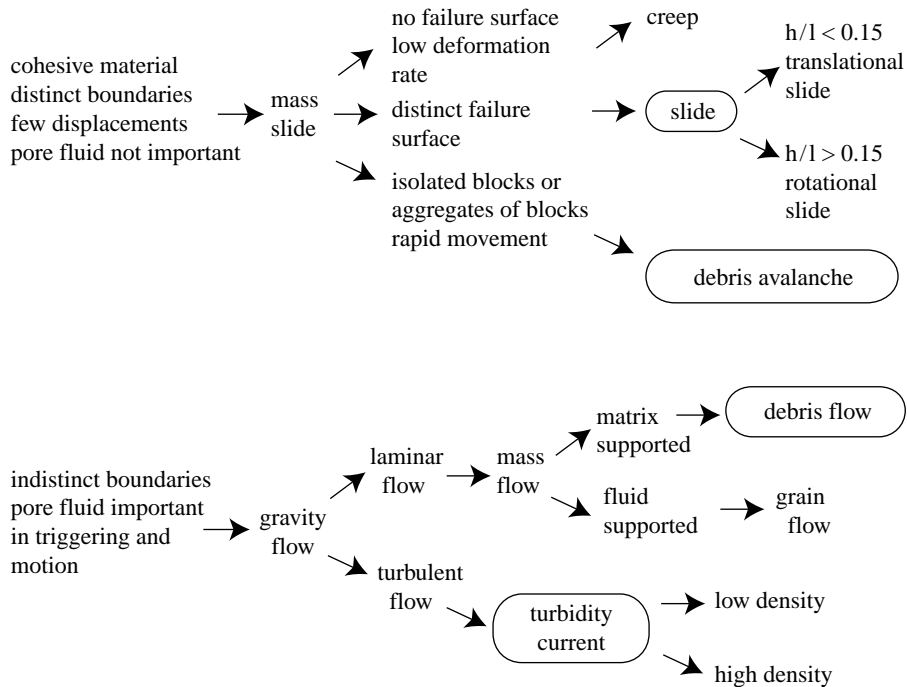


Figure 3. Summary classification of submarine landslide types (modified after [Mulder & Cochoat 1996](#)). The key flow types are highlighted. Slides, debris flows and turbidity currents are the main gravity-driven processes by which marine sediments are transported down slope. All have related hazards. Debris avalanches, although relatively rare in the submarine realm, are highlighted due to their specific hazard threat.

systems, to demonstrate that this concept was correct. Indeed, it seems that submarine landslides at all scales are often controlled in this way ([Lastras \*et al.\* 2004](#); [Wilson \*et al.\* 2004](#); [Bryn \*et al.\* 2005](#)). However, we know very little about the nature and characteristics of these weak layers, since they have rarely been sampled and very little geotechnical work has been done on sediments recovered from them. The weak layers that underlie parts of the Storegga slide are a notable exception ([Bryn \*et al.\* 2005](#); [Kvalstad \*et al.\* 2005](#)). Here it has been shown that the weak layers are composed of contourites (sediments deposited by ocean currents flowing along the continental slope) that are clay-rich and have higher water content and greater plasticity than the overlying less-well sorted glacial and glaciomarine sediments. As a result, the contourites are more sensitive and brittle (i.e. they lose strength rapidly when their strain bearing capacity is exceeded). Rapid loading of the water-rich contourites by glacial sediments appears to have raised pore pressures within the contourites and is the main factor contributing to landsliding.

Many sedimented slopes prone to submarine landslides show a history of landsliding that extends back through geological time. This observation can often be applied at quite local scales, with areas showing stacked landslide deposits sharply demarcated from those showing long-term stability ([Solheim \*et al.\* 2005](#)). The same is true of some volcanic island slopes, for example in the Canary islands, where part of the north flank of Tenerife has experienced at

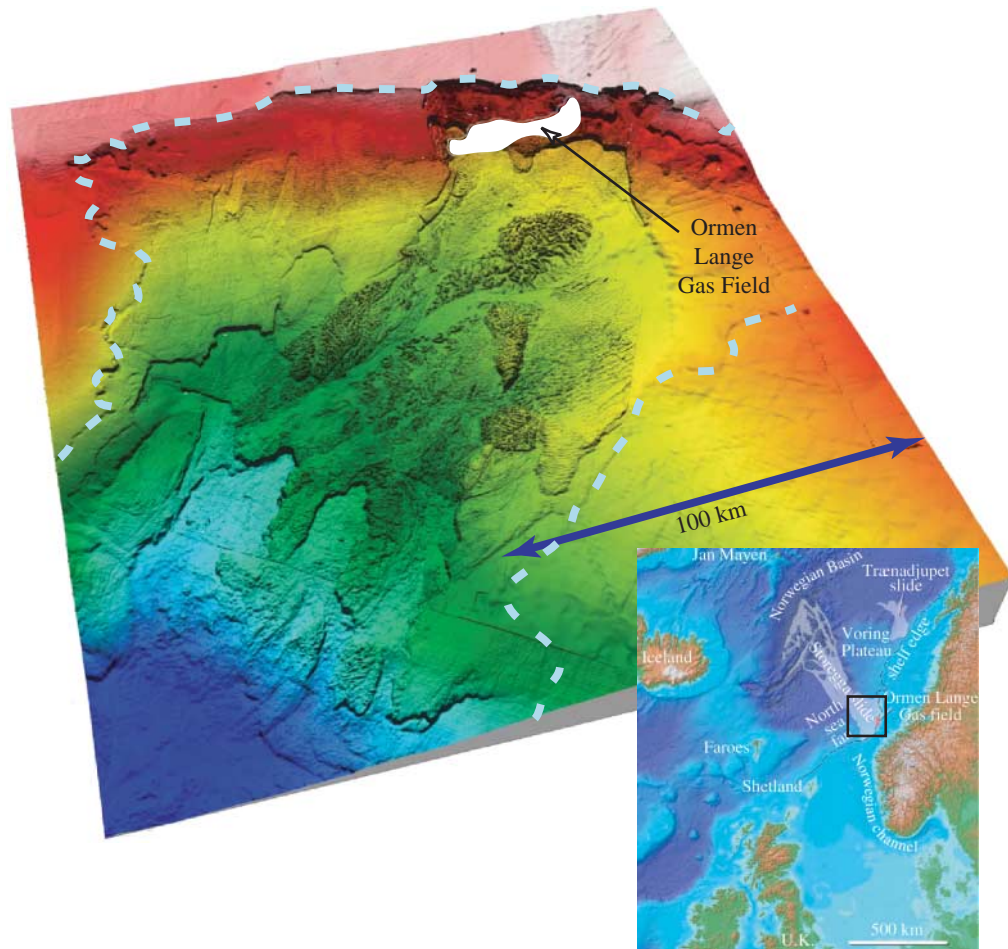


Figure 4. Three-dimensional image of the upper Storegga slide based on swath bathymetric mapping. Dotted line marks limits of landslide. Note the occurrence of multiple bedding-parallel failure planes (best seen bottom left) and the remnants of blocky landslide debris that partially fill much of the upper landslide scar. Image courtesy of Petter Bryn, Norsk Hydro.

least five landslides in the last 2–3 Myr, while adjacent regions have seen none (Masson *et al.* 2002). In a regional sense, repeated landsliding will be a natural consequence if the sediment deposition processes that generate the preconditions for landslides persist over long periods of time. Cyclic conditions, such as glacial/interglacial transitions may also contribute to repeated landsliding on timescales similar to the cyclicality (Bryn *et al.* 2005). One of the key reasons for repeated landslides at a site specific scale is that the scars created by landslides often act as traps for subsequent sedimentation, leading to enhanced sedimentation rates and increasing the risk of further landslides. Thus contourites are preferentially deposited in landslide scars on the Norwegian margin, enhancing weak layer development within these scars (Bryn *et al.* 2005; Solheim *et al.* 2005). Similarly, landslide scars in the Canary islands are frequently the loci of subsequent volcanism, probably because the landslide removes some of the overburden and creates an easier path for magma to reach

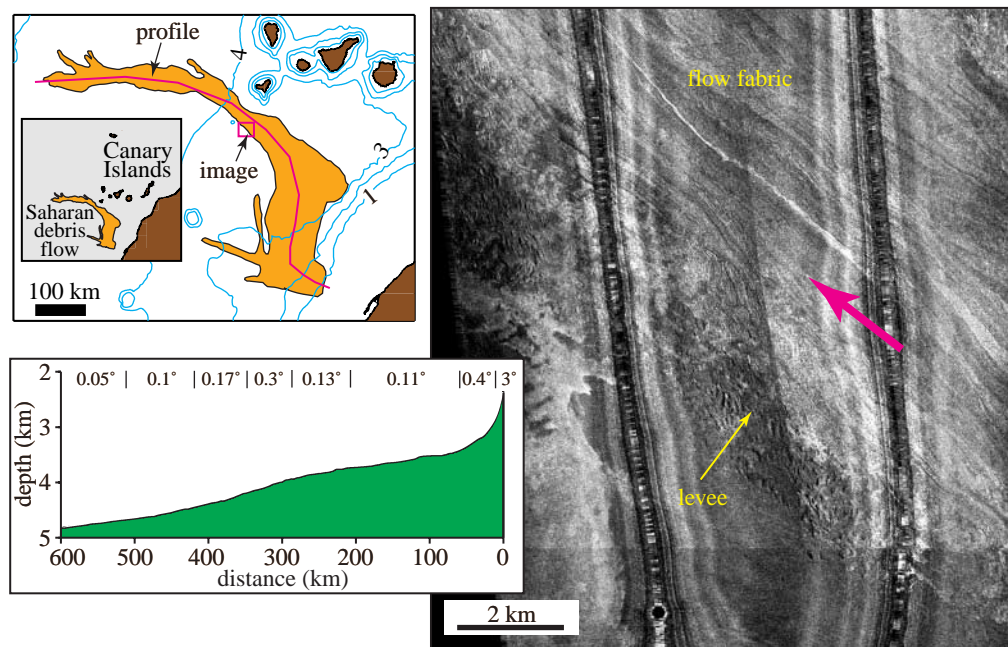


Figure 5. Location map, gradient profile along the axis of the landslide and sidescan sonar image of part of the Saharan slide, off west Africa. Magenta arrow indicates flow direction.

to the surface (Cantagrel *et al.* 1999). It is also possible that the debris left by a landslide, when loaded by subsequent volcanic products, can act as a weak layer for future landslides.

## 5. Landslide processes

Submarine landslides can be sub-divided into a bewildering variety of types (figure 3). However, in terms of volume of gravity-driven sediment transport in the ocean, only slides, debris flows and turbidity currents make a significant contribution (see §1 for definition of flow types). Debris avalanches are less significant in terms of total transport, but they pose a particular threat to human populations.

There is a generally accepted ‘paradigm’ that landslides in cohesive sediments evolve downslope from slide to debris flow to turbidity current through gradually increasing disintegration and entrainment of water (e.g. Mulder & Cochonat 1996; Iltstad *et al.* 2004; Bryn *et al.* 2005). However, this is probably an oversimplification in that some landslides travel many hundreds of km without appreciable transformation into turbidity currents, while others transform entirely into turbidity currents very close to source. In truth, the formation of large turbidity currents, in which a few hundred km<sup>3</sup> of (usually cohesive) sediment are rapidly mixed with much larger volumes of seawater, is a very poorly understood process (Talling *et al.* 2002).

Large landslides in continental margin sedimentary sequences are often complex events, and elements of slide, debris flow and turbidity current may all be evident in the aftermath of a single landslide. Often the slide scar will contain displaced but coherent slide blocks made up of sediments that have travelled

only a short distance from source (figure 4). Further downslope, the landslide deposit may show flow structures characteristic of debris flow processes (figure 5). A turbidity current initiated by the landslide may travel hundreds of km beyond the obvious limit of the debris deposit, with no obvious connecting pathway or deposit. In this situation the correlation between turbidite and landslide can often only be established on the basis of precise dating, sedimentology and/or geochemical analysis (Pearce & Jarvis 1992; Wynn *et al.* 2002).

Theoretical and experimental studies have shown that landslides on slopes as low as  $0.5^\circ$  are only possible where excess pore pressures at the level of the detachment surface support a large fraction of the weight of the landslide mass, thus decreasing the effective stress and the friction with the underlying substrate (Iverson 1997; Kvalstad *et al.* 2005). High pore pressures can be created through rapid sediment deposition (especially in fine-grained sediments with low permeability), collapse of the sediment structure (so-called 'sensitive clays') due to earthquake shaking, or possibly due to melting of gas hydrates contained within the sediment.

Debris avalanches occur when a mass of cohesionless material, usually fragmented rock, moves downslope. In the subaerial realm, debris avalanches typically occur on slopes that range from  $25^\circ$  to near vertical; in this situation they can attain speeds as high as  $100 \text{ m s}^{-1}$  ( $360 \text{ km h}^{-1}$ ; Voight & Pariseau 1978). The most widely known debris avalanches in the submarine realm are those that occur on the flanks of volcanic islands (Moore *et al.* 1989; Watts & Masson 1995; Ollier *et al.* 1998; Masson *et al.* 2002), although they also occur in consolidated sedimentary rocks on active continental margins due to failure of steep slopes generated by tectonic processes (Hühnerbach *et al.* 2005). On the submarine flanks of volcanic islands such as the Canary islands, debris avalanche failure planes dip oceanward at  $10^\circ$  or less, suggesting that these avalanches are less energetic than their subaerial counterparts. The blocky character of submarine debris avalanche deposits probably reflects the friable nature of the volcanic material and the distance of transport (typically an order of magnitude greater than the biggest subaerial avalanches) rather than the speed of the emplacement process. This is further discussed in §8.

## 6. The Storegga slide

As noted in a previous section, the Storegga slide, which occurred on the continental slope west of Norway around 8200 calendar years ago, is one of the largest and best-studied landslides on earth (Bugge *et al.* 1987, 1988; Hafidason *et al.* 2003; Hafidason *et al.* 2004; Bryn *et al.* 2005; Kvalstad *et al.* 2005).

The Storegga slide illustrates many key aspects of landslides on low angle continental slopes (figure 4). These include:

- (i) Several (at least 4) distinct gently sloping ( $0.5\text{--}2^\circ$ ) failure planes parallel to the sedimentary bedding.
- (ii) Steep ( $10\text{--}35^\circ$ ) headwall scarps separating the different glide plane levels.
- (iii) Landslide debris showing clear evidence of brittle deformation preserved in the landslide scar.
- (iv) Retrogressive behaviour.

An elegant geotechnical model for the Storegga slide was constructed by [Kvalstad \*et al.\* \(2005\)](#) who demonstrated that the best explanation for the slide required a combination of one or more weak layers, identified as marine clays (contourites) deposited during interglacial periods, and excess pore pressures developed as a result of the rapid sedimentation that loaded the Norwegian slope during intervening glacial periods. Evidence that high pore pressures existed in the area comes from measurements adjacent to the slide, where remnant high pressures can still be found. Modelling of the pore pressures found that excess pore pressure ratios of the order of 0.9 were required to cause failure. In simple terms this means that the strength of the sediment was reduced to about 10% of its normal level. There is clear evidence that instability only developed at certain levels in the sediment and that consequently most of the sediment pile was inherently stable. This is best seen on high-resolution seismic data that show faulted and fractured slide debris preserved within the slide scar ([Kvalstad \*et al.\* 2005](#)). It is also shown by the long term stability of the steep slide headwall scarps, which have stood with angles of up to 35° for over 8000 years since the excess pore pressure in the weak layers was released by the landslide.

The area of the Storegga slide shows a long-term history of sedimentation and landsliding that reflects glacial/interglacial cyclicality ([Solheim \*et al.\* 2005](#)). This leads to the conclusion that the state of stability that has characterized the Storegga slide area since the last landslide occurred is unlikely to change until the next interglacial/glacial cycle has been completed.

## 7. Canary island landslides

Large-scale landslides are a common feature of volcanic ocean islands such as Hawaii, the Canary islands and Reunion island ([Moore \*et al.\* 1989, 1994](#); [Watts & Masson 1995](#); [Masson 1996](#); [Ollier \*et al.\* 1998](#); [Masson \*et al.\* 2002](#)). The Nuuuanu landslide, off Oahu in the Hawaiian islands, with an estimated volume of 5000 km<sup>3</sup>, may be the largest single landslide on earth ([Moore \*et al.\* 1989](#)). Landslides on volcanic islands typically take two forms—debris avalanches and slumps (in the terminology used in this paper a slump is a type of slide). As defined by [Moore \*et al.\* \(1989\)](#), a debris avalanche is a relatively thin (0.4–2 km thick) landslide with a clear evacuated headwall and a distal train of blocky debris. Each debris avalanche appears to be a single event, at least in terms of geological time, and some show evidence for rapid and energetic emplacement. In contrast, a slump involves gradual, intermittent, downslope movement of a thick (up to 10 km) coherent block of the island flank.

The history of landslides in the Canary islands over the past one million years is now well understood (see [Masson \*et al.\* \(2002\)](#) and references within). The bulk of landslide activity is associated with the youngest and most volcanically active islands of Tenerife, La Palma and El Hierro ([figure 6](#)). On average, one landslide has occurred somewhere in the Canary islands every 100 000 years, although this figure masks an irregular distribution through time ([Masson \*et al.\* 2002](#)). The youngest landslide occurred on the island of El Hierro some 15 000 years ago. Most of the landslides are debris avalanches, with slumps only recognized on the youngest island, El Hierro, perhaps suggesting that this landslide style is a feature of early island development. A typical Canary island debris avalanche is

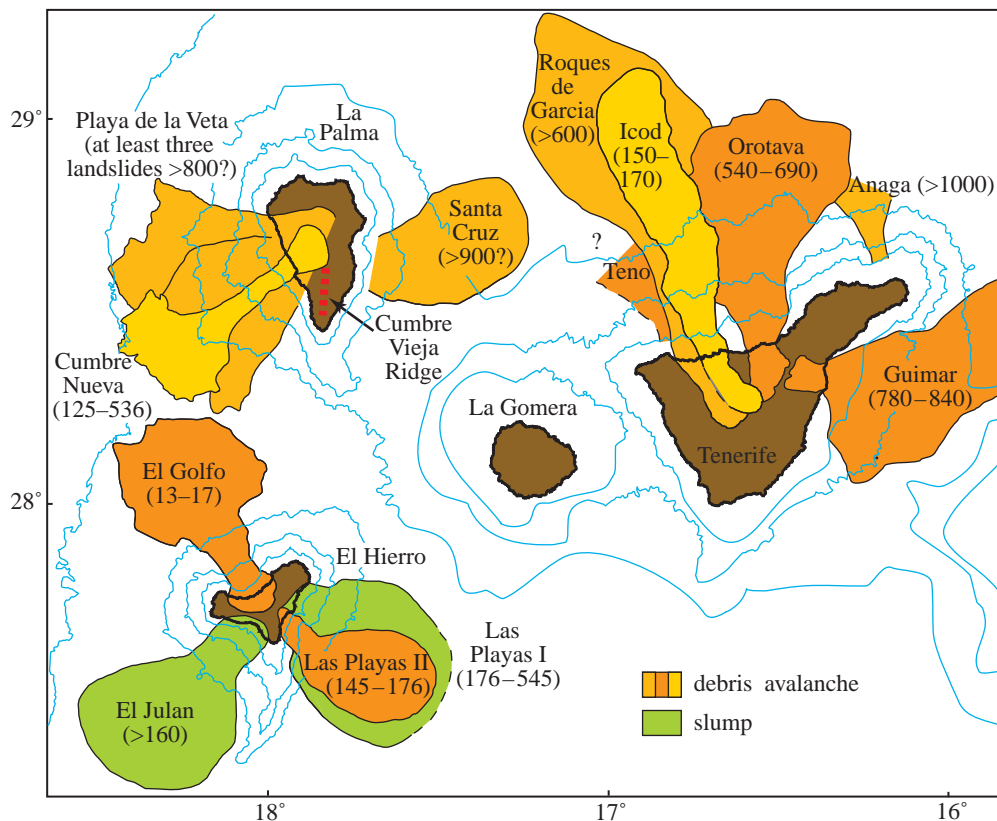


Figure 6. Location and ages (in brackets) of large landslides on the western Canary islands. The Cumbre Vieja Ridge is recognized as the likely site of a future landslide.

marked by a near-vertical amphitheatre-shaped headwall on the island, an erosive chute on the upper part of the submarine island slope and a pile of avalanche debris at the foot of the steepest island slope, usually at 3000–4000 m waterdepth (figure 7). This typical avalanche has a volume of 50–200 km<sup>3</sup>, covers an area of a few thousand km<sup>2</sup> and has a run-out of 50–100 km. Glide planes at the base of the landslide are typically up to 10° on the upper slope, decreasing to less than 5° on the lower slope (Watts & Masson 1995; Gee *et al.* 2001; Watts & Masson 2001). Large accumulations of debris, such as seen north of Tenerife or west of La Palma, are clearly the cumulative result of several landslides rather than single larger events that have occurred in the past. Even some deposits thought to be the result of a ‘single’ landslide event (in geological time) show signs of more than one phase of emplacement (Watts & Masson 2001). It is notable that Canary island debris avalanches are an order of magnitude smaller than those on Hawaii, possibly reflecting the larger size and higher magma production rates of the Hawaiian islands or the more rapid development of instability on the relatively steeper Canary island slopes.

Canary island landslides identified as debris avalanches according to the definition of Moore *et al.* (1989) show a variety of structures that suggest elements of both debris avalanche and debris flow emplacement mechanisms

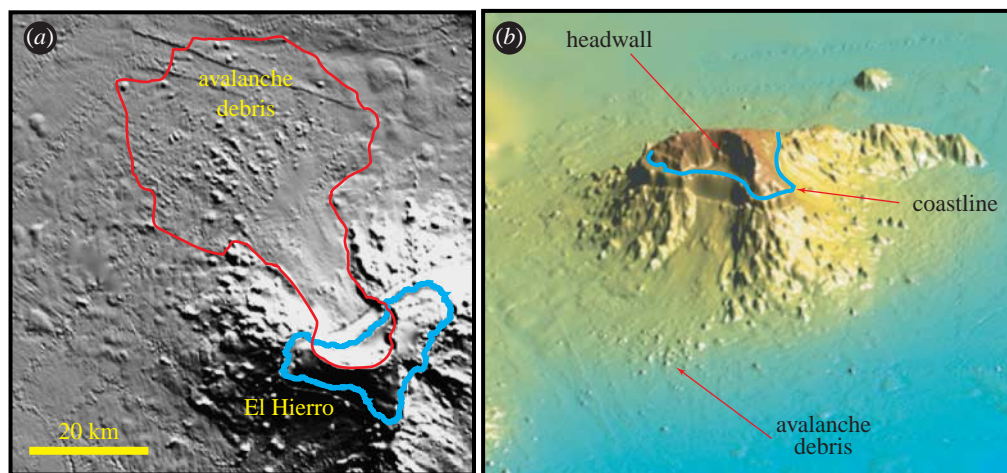


Figure 7. Two views of the El Golfo debris avalanche on the island of El Hierro, western Canary islands (for location see figure 6). (a) Shows a plan view shaded relief image, illuminated from the northeast. The limits of the area affected by the landslide are outlined in red. Note that avalanche blocks are scattered randomly on the landslide, although there is a notable concentration of blocks in the centre of the deposit. (b) Shows an oblique shaded relief model viewed from the northwest. The avalanche headwall on the island is about 1000 m high.

(figure 8; Masson *et al.* 2002). In addition, these landslides can also initiate turbidity currents that are capable of flowing considerable distances downslope. Sediment cores recovered from the deep Agadir Basin, about 300 km to the north of the islands, contain turbidite deposits which, based upon their mineralogy, geochemistry and age, are interpreted to be linked to Canary island landslides (Wynn *et al.* 2002; Wynn & Masson 2003). Specifically, a turbidite deposited at  $\sim 15$  kyr is linked to the El Golfo landslide on El Hierro, while an older turbidite dated at *ca* 170 kyr is linked to the Icod landslide on Tenerife. Most turbidite deposits in the Agadir Basin are actually derived from the Moroccan continental margin to the east (Wynn *et al.* 2002), and show the typical smooth upward-fining grain-size profile that is typical of graded turbidite deposits (figure 9). However, the two turbidites derived from Canary islands landslides show a stepped grain-size profile that appears to represent deposition from a series of ‘mini-turbidites’ (figure 9). This pattern is interpreted to be the result of a multi-stage source landslide, as other potential causes, e.g. flow reflection, multiple pathways or pulses, can be ruled out (Wynn & Masson 2003). This hypothesis is also supported by the fact that similar turbidites linked to Hawaiian landslides show the same pattern of stacked mini-turbidites (Garcia 1996). Detailed sedimentological analysis of the Agadir Basin turbidites has revealed that their source landslides probably occurred in several retrogressive stages over a period of hours or days rather than weeks or months (Wynn & Masson 2003). Assessing the sedimentary record of deposits derived from these landslides is therefore critical when assessing their tsunamigenic potential, since it is clear that a series of smaller landslides spread over several hours will have a much smaller tsunami-building potential than a single large, instantaneous landslide (see §8).

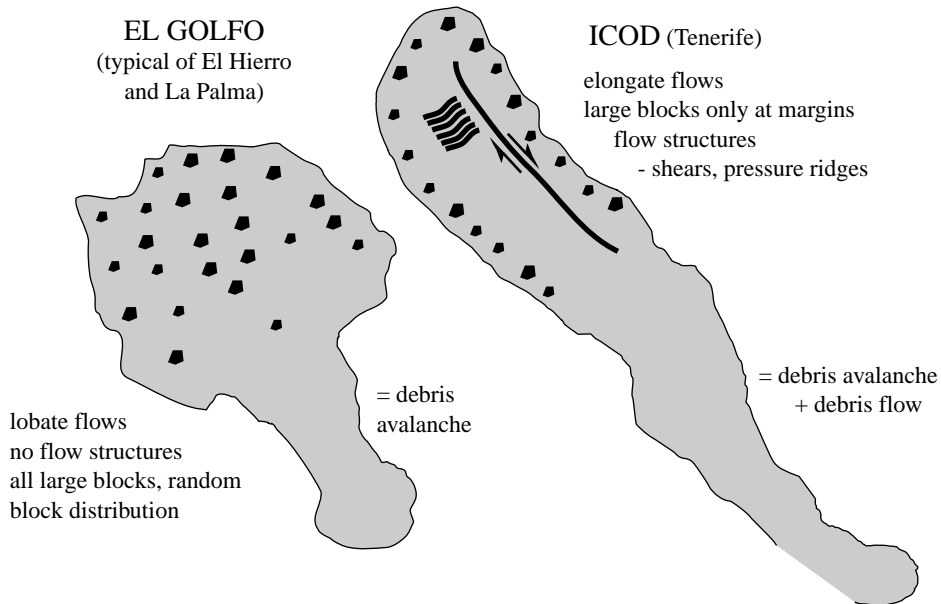


Figure 8. Summary of the end members of the group of Canary island landslides classified as debris avalanches (based on data presented in Masson *et al.* 2002). This shows elements of cohesive debris flow as well as cohesionless flow (avalanche). Given the low angle glide planes on which these landslides moved it seems likely that both the landslides began as slides, with the debris avalanche morphology reflecting only the disintegration of the mass of friable basaltic rocks in the slides as they moved down slope.

## 8. Landslide-generated tsunamis

The generation and propagation of tsunamis resulting from earthquakes have been studied for the last 50 years and are now relatively well understood (Bardet *et al.* 2003). In contrast, the importance of tsunamis generated by landslides has only become widely recognized during the last fifteen years or so, when it became apparent that a landslide source could explain the unusual run-up distributions and propagation characteristics of certain particularly deadly tsunami, such as the 1998 PNG event (Ward 2001; Bardet *et al.* 2003 and references therein; Okal & Synolakis 2004). However, the complexity and variability of submarine landslides means that we are still some way from a comprehensive understanding of the range of tsunamis that landslides are capable of producing. Modelling of landslide tsunamis has shown both that extreme wave heights of hundreds of metres might be possible (Ward & Day 2001; McMurty *et al.* 2004), but that models are sensitive to the geological input parameters and the hydrodynamic assumptions adopted in the model (Ward 2001; Haugen *et al.* 2005; Lovholt *et al.* 2005), with the result that poorly constrained model predictions will have large uncertainty.

Despite the variability of submarine landslides that might cause tsunamis, many such tsunamis show similar general characteristics. In particular, these tsunamis often have very large run-ups close to the landslide site but appear to propagate much less efficiently than earthquake tsunami, so have limited far-field

effects (Okal & Synolakis 2004). This was exemplified by the 1998 PNG tsunami, where waves up to 15 m high affected a 20 km segment of coast, killing 2200 people (McSaveney *et al.* 2000) even though farther a field the tsunami was not a significant event (Okal & Synolakis 2004). This is a consequence of the relatively small source areas of most landslide tsunami (compared to the areas affected by large earthquakes) that leads to the generation of shorter wavelength waves. These are more prone to coastal amplification (increasing the local effect) and to radial damping (decreasing the distal effect). This contrasts with the lack of radial damping seen in earthquake tsunamis that are generated by elongate two-dimension sources; these tsunamis propagate perpendicular to the source fault with little radial spreading.

The tsunami generated some 8200 years ago by the Storegga slide off Norway is one of the best-understood landslide tsunamis. A well-preserved record of tsunami deposits on land in Norway, Scotland and the Faroe islands (Dawson *et al.* 1988; Bondevik *et al.* 1997, 2005) coupled with an unprecedented knowledge of the landslide processes (Bryn *et al.* 2003, 2005; Haffidason *et al.* 2003, 2004; Kvalstad *et al.* 2005), provides the basis for rigorous testing of tsunami models and allows the key landslide parameters to be identified (Bondevik *et al.* 2005; Haugen *et al.* 2005; Lovholt *et al.* 2005). The key findings are that landslide volume, velocity, initial acceleration, length and thickness all contribute to the determination of tsunami character. The best indicator of tsunamigenic potential is the product of volume and initial acceleration (Lovholt *et al.* 2005). An abrupt deceleration might also contribute to larger surface elevations. The slide length affects both the wavelength and the maximum surface elevation (Haugen *et al.* 2005), while the wavelength is also determined by the travel time or run-out distance of the slide. Submarine slides are normally clearly subcritical, i.e. the Froude number (the ratio of slide speed to the speed of wave propagation) is much less than one. This implies that the tsunami will run away from the wave-generating slide, limiting the build-up of the wave. Slides in shallow waters are more critical, since the speed of wave propagation is lower here. Moreover, shallower water normally means less distance to the coast and a shorter distance available for radial damping. In contrast, tsunamis generated by earthquakes are more critical when the seabed displacement occurs in deeper waters, as the initial wave (which in this case depends much less on the water depth) will become shorter and more dangerously amplified when propagating from deeper to shallower waters.

The Storegga slide is best modelled as a retrogressive slide, with a peak velocity of 25–30 m s<sup>-1</sup> (Bondevik *et al.* 2005). The retrogressive slide, of total length  $L$ , is modelled as a train of  $N$  fixed block slides released at different times  $t$ , but moving with identical velocity distributions (Haugen *et al.* 2005). For simplicity, the blocks have the same thickness  $h$  and the same length  $L/N$ . Moreover, the time lag  $\Delta t$  between release of two adjacent blocks is assumed to be equal. For waves propagating in the same direction as the slide, increasing  $\Delta t$  increases the distance between the surface elevations caused by the individual block modules. This decreases the overlap and results in a smaller amplitude and longer wave (figure 10). For small time lags, the wave remains smooth, but as  $\Delta t$  increases, the distances between the individual block modules become large and the discrete nature of the retrogressive slide starts to show. Eventually, when  $\Delta t$  is sufficiently large, the waves generated by the block modules are completely separated.

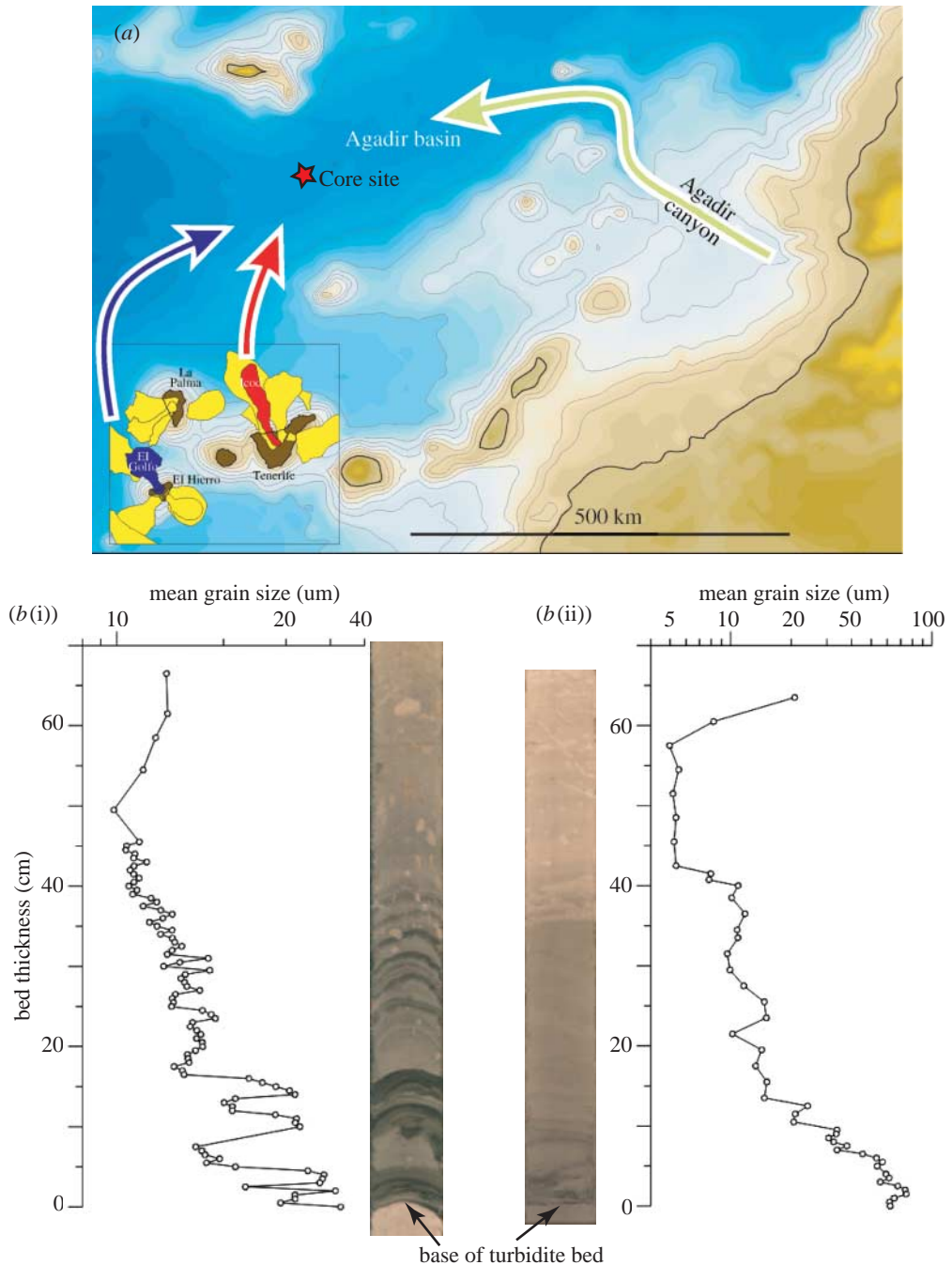


Figure 9. (Caption opposite.)

The waves moving in the opposite direction of the block modules also move in the same direction as the retrogressive process. Thus, small time lags will decrease the distance between the surfaces elevations caused by the individual block modules. Consequently, the overlap increases, resulting in a larger

Figure 9. (*Opposite.*) (a) Location of the Agadir Basin north of the Canary islands; some 50 piston cores have now been collected in the basin. The pathways along which turbidity currents related to landslides on El Hierro (blue) and Tenerife (red) travelled to the basin are indicated. (b) Two sections of sediment core from the Agadir Basin, showing the appearance and grain size profile of a turbidite associated with a landslide on (b(i)) the Canary islands and one derived from (b(ii)) the African margin. The main difference is that the Canary island turbidite consists of a stacked sequence of fining-upwards beds (black represents concentrations of relatively coarse volcanoclastic minerals) interpreted as a sequence of flows emplaced over a period of hours to days, while the African margin turbidite is a single fining-upward sequence emplaced in a single flow. This indicates that Canary island landslides are relatively slow, probably retrogressive, failures rather than single instantaneous events (see text for further details).

---

amplitude but shorter wave. When the time lag equals the time it takes for the wave to traverse a block module, i.e.  $\Delta t = L/N(gH)^{-1/2}$ , where  $H$  is the water depth, the individual surface elevations interfere in a perfectly constructive manner and the amplitude is at its maximum. As the time lags are increased further, the waves moving in the opposite direction of the block modules exhibit the same dependence on  $\Delta t$  as described above for the wave moving in the same direction as the slide.

Models of the Storegga slide indicate that retrogression must have been rapid, taking less than one hour; slower retrogression cannot reproduce the observed tsunami run-up pattern. Bondevik *et al.* (2005) compared field observations with run-up heights deduced from new numerical simulations of the Storegga slide tsunami (figure 11). The shape and volume of the slide were adjusted to new and more detailed reconstructions of the slide (Forsberg 2002; Hafidason *et al.* 2005). In the revised slide model the maximum thickness (400 m) of the slide is near the upper headwall and it becomes gradually thinner towards the slide front in the offshore direction. The slide is modelled as a box that is skewed and smoothed to reproduce the reconstructed morphology of the Storegga slide, and moves with maximum velocities of 20–35 m s<sup>-1</sup>. All simulations use a run-out distance of 150 km. A linear, long wave numerical model simulates the tsunami. A maximum velocity between 25 and 30 m s<sup>-1</sup> with a 25% reduction of the surface elevation due to landslide retrogression makes the best match to the field observations (Bondevik *et al.* 2005). According to a two-dimension retrogressive slide model (Haugen *et al.* 2005), such a reduction is obtained with a very little time lag, about 15–20 s between the sliding blocks. Velocities of 25–30 m s<sup>-1</sup> are also supported by De Blasio *et al.* (2005), who find mean (centre of mass) slide velocities of 25–35 m s<sup>-1</sup> in their run-out studies of the Storegga slide.

Ward & Day (2001) modelled a tsunami generated by a landslide on the west flank of La Palma island in the Canaries. These authors concluded that for a worst-case scenario an initial wave elevation of up to 900 m could be generated by a landslide of 500 km<sup>3</sup> volume that reached a peak velocity of 100 m s<sup>-1</sup> after 2 min of travel, i.e. with an acceleration of almost 1 m s<sup>-2</sup>. This tsunami would have the capability to cross the Atlantic, producing a 10–25 m high wave along the east coast of North America. However, Ward & Day (2001) use a linear dispersive model that does not describe nonlinear effects and wave breaking. Hence, the initial waves may be overestimated and the wave spectrum could contain too great a proportion of short wave components experiencing the strongest amplification and producing the highest run-up. We note that similar

conclusions have been reached by other authors (e.g. Mader 2001) who provide estimates of wave elevation along the North American coast an order of magnitude smaller than those calculated by Ward & Day (2001).

As noted for the Storegga slide, tsunami wave elevation is strongly influenced by landslide volume (or by some combination of landslide frontal area, length and thickness), by peak velocity, and by initial acceleration. For the La Palma scenario Ward & Day (2001) used maximum possible values for these parameters, adopting a 'worst-case' geological scenario as their model input. However, geological understanding of Canary island landslides, especially the offshore deposits, provides a number of reasons for challenging the models of Ward & Day (2001). These include questions of landslide process, volume and velocity. In terms of landslide failure processes, the scars left on the islands give few clues. However, they do allow the slopes of the glide planes on which the slides occurred to be measured. Even the steepest of these, on the upper slope of the El Golfo landslide off the island of El Hierro, only reaches a maximum of  $10^\circ$ , decreasing to about  $5^\circ$  at the base of the island flank where the avalanche deposit begins (Gee *et al.* 2001). Further offshore, key features of the landslide deposits suggest that both debris avalanche and debris flow processes are involved in landslide emplacement (figure 9). The question of what this debris avalanche morphology actually tells us about the emplacement process, and particularly about the velocity of the landslide, is clearly important. Unfortunately, the term debris avalanche immediately brings to mind the rapid, catastrophic rock avalanches that occur in mountain ranges on land (Voight & Pariseau 1978). These can reach velocities in the order of  $100 \text{ m s}^{-1}$  on slopes that range from  $25^\circ$  to near vertical (Plafker & Ericksen 1978; Voight & Pariseau 1978). However, it is difficult to envisage this type of process for Canary island debris avalanches, where the slide plane gradients are less than  $10^\circ$ . Here it seems likely that the debris avalanche morphology reflects the disintegration of a slide composed of brittle volcanic rock and therefore primarily reflects the non-cohesive character of the slide material. In this situation, it probably tells us little about the velocity of the landslide.

Nevertheless, general considerations of submarine landslide behaviour leads us to predict that Canary island landslides must be relatively energetic, so peak velocities in the order of  $50 \text{ m s}^{-1}$  need to be considered in tsunami modelling. This is supported by evidence from the Ritter island volcano collapse, where velocities of  $40 \text{ m s}^{-1}$  have been modelled on the basis of known landslide volume and tsunami run-up heights (Ward & Day 2003) and from offshore Hawaii, where debris avalanches that run-up the far side of the islands' flexural moat require velocities in the order of  $80 \text{ m s}^{-1}$ . Using the scaling arguments of Ward & Day (2003), Canary island landslides might be expected to have velocities intermediate between those of the above examples, although given that the glide plane for the Ritter island landslide ( $10\text{--}25^\circ$ ) is considerably steeper than glide planes in the Canaries ( $5\text{--}10^\circ$ ),  $50 \text{ m s}^{-1}$  might be considered a maximum for Canaries examples. This is still well below the velocity at which the tsunami would propagate in the deep water west of the Canary islands, so little coupling between the landslide and the tsunami would occur. The initial acceleration of the landslide is even less well constrained than the peak velocity, but is just as critical in determining the tsunami-generating potential of a landslide (Haugen *et al.* 2005). Ward & Day (2001)

used an extremely high acceleration,  $0.83 \text{ m s}^{-2}$ , in their La Palma model. This is 50 times higher than the acceleration that produced the best-fit model for the Storegga slide (Lovholt *et al.* 2005) and appears unlikely on a glide plane of  $10^\circ$  or less. To put it in context, a landslide acceleration of  $0.83 \text{ m s}^{-2}$  is about half of what would act on a subaerial block on a  $10^\circ$  plane with zero friction or resisting forces, such as the need to displace the water that forms the tsunami ( $a = g \sin 10^\circ = 1.70 \text{ m s}^{-2}$ ).

Questions regarding the volume of any future landslide from La Palma, and about the way in which it would fail, are perhaps the most critical in determining the size of the modelled tsunami. Ward & Day (2001) used a volume of  $500 \text{ km}^3$  in their calculations with the assumption that this failed as a single block. However, this volume is two to three times bigger than a typical Canary island landslide, even though the area affected by their potential landslide is quite typical. This is because they assume a failure surface ‘2–3 km below the summit of the volcano’ (Ward & Day 2001), despite the fact that reconstruction of other landslides on the Canary islands, supported by the offshore debris flow volumes, show their maximum thicknesses to be in the order of 1–1.5 km (Urgeles *et al.* 1997; Masson *et al.* 2002; Hurlimann *et al.* 2004). Most importantly, observations of turbidites associated with Canary island (and Hawaiian) landslides show that they did not fail as single blocks, and that the separation in time of the phases of the multi-stage failures was almost certainly sufficient to separate their tsunami-building potential (see §7).

In summary, we would suggest that many of the parameters used in the worst-case scenario for a future landslide from the island of La Palma, as modelled by Ward & Day (2001), have been pushed to, or often beyond, their feasible maximum values. Any future tsunami is thus likely to be smaller than the Ward and Day prediction. Furthermore, it needs to be recognized that the worst-case landslide is in any case an unlikely event, with a probability much smaller than the 1 in every 100 000 years re-occurrence time calculated overall for Canary island landslides. Nevertheless, we can be certain that future landslides will occur in the Canaries. It is also probable that such an event will generate locally devastating tsunamis, with run-ups exceeding anything seen in historical tsunamis elsewhere. However, the ability of such landslides to produce significant trans-oceanic tsunamis is much more questionable.

## 9. Prediction and risk assessment

The prediction of landslides in the submarine realm, where any precursor movements cannot generally be observed, is problematic—we know in general where landslides occur (and will occur) but we are far from being able to provide reliable forecasts of individual events, especially where the final trigger is likely to be a transient event, such as an earthquake, which in itself cannot be predicted. On land, areas of particular risk, e.g. the west flank of La Palma in the Canary islands, can be monitored using seismometers or GPS arrays to warn of ground movement, but it is not practical to monitor all but the most high risk areas onshore, and almost impossible to monitor offshore areas. On human timescales, understanding how seabed exploitation, such as oil and gas exploration and production, might contribute to slope failure and landsliding is

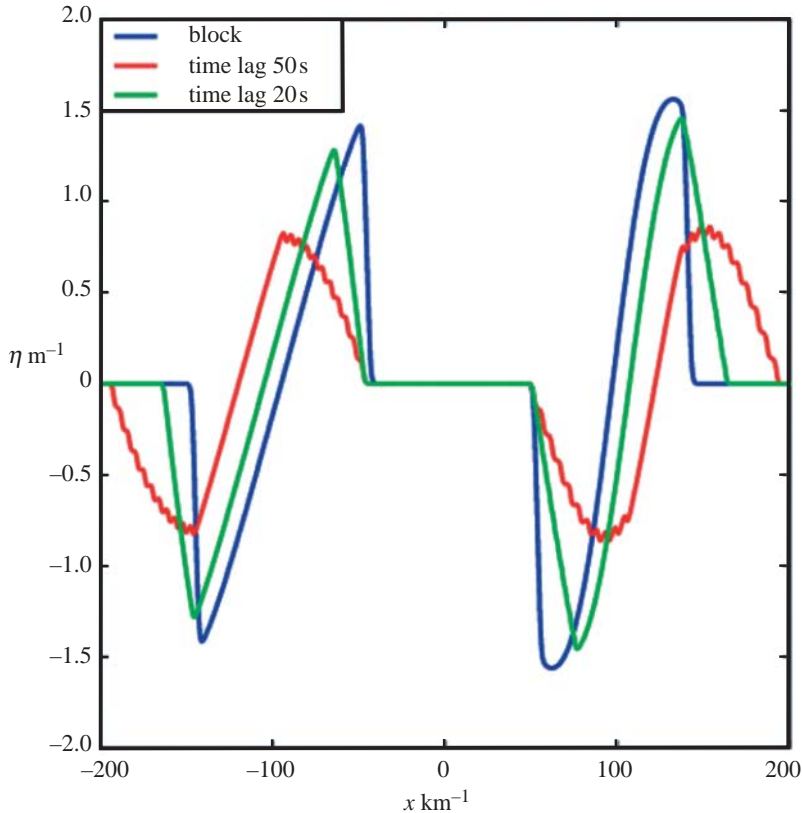


Figure 10. Three plots showing how the shape of the surface waves varies with time lag  $\Delta t$  in a retrogressive landslide. An ocean depth of  $H=1000$  m is assumed, and the retrogressive landslide consists of  $N=11$  block modules, each of height  $h=20$  m and length  $L=400$  m. The individual module has a sinusoidal velocity distribution  $u(t)$  with maximum velocity  $u_{\max}=10$  m s $^{-1}$  and run-out distance  $R=6$  km. Note that the wavelength increases while the amplitude decreases with increasing time lag  $\Delta t$ . Also note how the discrete nature of the retrogressive slide process is visible when  $\Delta t=50$  s. These two-dimensional calculations were carried out by K. B. Haugen, NGI.

of current importance. The huge effort made to understand the Storegga slide, and the cost of this effort, demonstrate that even past landslides can be a significant financial hazard in the offshore industry.

The 2004 Indian Ocean tsunami was a reminder of the power of this natural phenomenon and that such events, created by landslides as well as earthquakes, have a worldwide distribution. Early warning systems for tsunamis are useful on a short time scale. On a longer time scale, we can only attempt to manage the consequences. Here, a probabilistic analysis of tsunami hazard is essential for estimating the potential losses and risk to human life and infrastructure along the coastline. The development of a Probabilistic Tsunami Hazard Analysis (PTHA) tool should follow the same lines as the Probabilistic Seismic Hazard Analysis (PSHA), which has become standard practice in the evaluation and mitigation of seismic hazards to structures, infrastructure and lifelines. The ability of PSHA to condense the complexities and variability of seismic activity into a manageable set of parameters greatly facilitates the design of effective

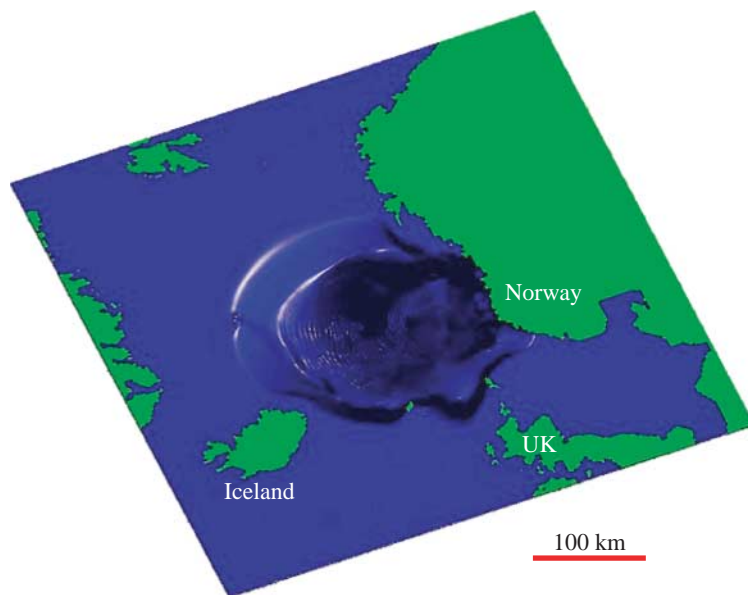


Figure 11. Numerical simulation of the Storegga landslide tsunami 90 min after the initiation of the landslide. This model successfully reproduces the known tsunami run-up heights in Norway, Scotland and the Faroe islands.

seismic resistant buildings and infrastructure. The PTHA tool should be designed to provide a synopsis of the tsunami hazard along entire coastlines and identify the specific tsunami source regions that most strongly influence the tsunami hazard at each site on the coastline.

Because submarine landslides are rare on a human timescale, unpredictable, and almost impossible to observe and instrument, numerical modelling is seen as one of the key ways forward, both for understanding the landslides themselves and for the prediction of landslide tsunamis. Aspects of modelling are discussed in the following two sections.

## 10. Numerical modelling of landslide dynamics

Submarine landslides may have huge dimensions and long run-out distances. Modelling the entire three-dimension problem is a huge computational task, and usually has to be reduced to a two-dimension problem through depth averaging or through restriction to cross sections to save computation resources. The loss of information about the vertical profiles of the velocity and density is usually insignificant, in particular for large-scale events. However, even a two-dimension simulation is a non-trivial task for large landslides. If it is known that the lateral spreading of the flowing mass is weak or limited, the flow evolution in the transversal direction may be neglected and one-dimension models may be applied.

Models should preferably describe the multi-layer structure of a submarine landslide with a dense debris flow at the bottom and a dilute turbidity current (suspension flow) above it. Hence, the vertical density variations and the associated variation of the mechanical properties should be taken into account.

The dense debris flow is often considered either as a saturated mass of cohesionless material, or as a visco-plastic material where no deformation takes place until a specified stress is applied to the material, after which deformation is driven by the excess of the stress beyond the yield stress. An example is the frequently used Bingham fluid model, describing a viscous Newtonian fluid combined with a yield stress. Such a fluid moves as a dense plug flow riding on top of a shear flow. Material properties, including clay rheology, are of great importance to the flow dynamics and travel distance for the majority of events. The material properties also affect the rate of erosion and channelization. In the dense layer, energy dissipation is due to particle–particle interaction in granular flows with high particle concentrations, and to viscosity for more fluidized flows with lower particle concentration. Clay slurries exhibit yield strength threshold behaviour and viscosity, not only for (visco-plastic) shear flows, but also in extensional flows.

In modelling of failure and rupture, the separation of two material volumes that were originally adjacent poses specific problems. In simulating the evolution of a sliding block at the escarpment during the retrogressive phase of the Storegga slide, the progressive decay of the original slab into wedge-shaped blocks had to be reproduced (figure 12). Two key factors in the model were responsible for the emergence of shear bands at the correct places (i.e. as observed in high-resolution profiles across the landslide), namely the assumption of shear softening and the high-resolution grid. All time- and location-dependent material properties such as the yield strength had to be advected with the flow, requiring substantial computing resources.

For engineering purposes, knowledge of impact loads is needed for both granular, visco-plastic and suspension flows. Depth-averaged (hydraulic) models may simulate high-Froude number granular flows against obstacles quite well (applying appropriate shock-capturing numerical schemes). For suspension flows with Froude numbers close to 1, the assumption of hydrostatic pressure distribution in the hydraulic models is poor in the head of the current where the largest pressures have to be expected, and complex two-dimension or three-dimension models may have to be used. The situation is less clear for visco-plastic flows because the rheology is only partially known, and because determination of yield surfaces will be involved. Today, it is not known whether two-dimension (depth-averaged) models are applicable when the yield strength is important.

## 11. Numerical modelling of landslide tsunamis

The quantitative description of gravity mass flows poses a series of nontrivial problems linked to stability, rheology, disintegration and mixing with water during landslide propagation. In addition, modelling of the tsunami, in particular close to the source region, requires an approach different to that used in modelling tsunamis generated by earthquakes. The open sea propagation of earthquake tsunamis is most commonly described by the shallow water equations that are the simplest member of the class of depth integrated long wave equations. Even though errors due to frequency dispersion may accumulate in trans-oceanic propagation and that certain phenomena in shallow water as well as details in the generation are lost, the shallow water equations are generally

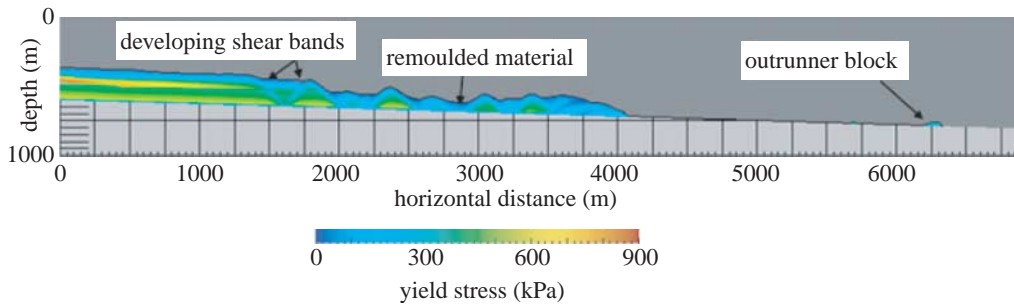


Figure 12. Simulation of slab evolution in a retrogressive slide with the Eulerian finite-volume code CFX-4. The yield stress at an intermediate time (1 h 25 min) is shown. Strain softening as a function of the accumulated shear was implemented in a Bingham rheology. Note the shear bands separating the wedge-like glide blocks and the outrunner block. Courtesy P. Gauer, NGI.

adequate for this purpose. Moreover, the final seabed elevations from the earthquake are transferred to initial elevations on the ocean surface. As a rule this simple practice does suffice.

For submarine slides the corresponding simple source model is an equivalent sink/source distribution with prescribed shape and motion. However, this is indeed a crude model for submarine slides, for which the interaction between the solid constituents of the flow and the fluid may be crucial both for the slide dynamics and the generation of the tsunami. For rock-type slides depth integrated wave equations may still be used in combination with corresponding slide models, maybe with parameterization of features like exchange of fluid between the slide body and the surrounding fluid. On the other hand, mud type mass gravity flows will entrain water, and produce turbulence and large vortices, while form drag may have a crucial influence on the shape and dynamics of the mudflow. For slides with a subaerial origin the impact in water and progression in shallow depths involve wave breaking and huge wave resistance (momentum exchange with surface gravity waves in the water). Another challenge is the retrogressive slide dynamics (see §8), where the tsunami generation by a series of smaller slide masses clearly calls for hydrodynamic analysis and modelling beyond long wave assumptions. In short, a proper quantitative description of mass gravity flows and their tsunami generation requires general hydrodynamic computational tools, like Navier–Stokes type models, but with modified rheology for the denser types of slide masses. Today, three-dimension models of this kind are so computationally demanding that simulations with sufficient resolution are difficult to perform even on the most powerful computers.

Assuming that an appropriate model is available for the mass gravity flow and the generation of surface waves, the far-field tsunami propagation still has to be handled with some set of depth integrated, long wave equations, that must be coupled with the more complex model for the source region. In many cases the vicinity of the slide will be dominated by flow structures associated with vortices and turbulence that cannot be conveyed properly to a depth integrated model. In comparison to the energy and momentum following the tsunami, these features are advected much more slowly by the material fluid velocity. Hence, the simplest option would be to employ a large source region that allows the transition of pure waves to the depth integrated far field. However, this will be

difficult to achieve due to computational limitations. Presumably, the wave motion must be identified and extracted in the vicinity of the slide, which is far from straightforward.

Mass gravity flows frequently occur in the aftermath of an earthquake, causing tsunamis additional to and much more localized than those from the earthquake itself, but at the same time potentially very destructive (Bardet *et al.* 2003; Okal & Synolakis 2004). Moreover, the wavelengths may occasionally be much shorter than for tsunamis of seismic origin, which implies that a dispersive model must be used (Lynett *et al.* 2003). The complete modelling of the mass gravity flow and the generation and propagation of the tsunami may require an optimal application and combination of a diversity of hydrodynamic models. Both the combination of computational tools and the need to parallelize the heavy computations point to a domain decomposition strategy. Such techniques, together with related techniques on nesting have been applied for a while, but more development and testing are needed, in particular for the combination of genuinely different models.

## 12. Summary and conclusions

Landslides are ubiquitous features of submarine slopes in all geological settings and at all water depths. Because of their unique geological settings, submarine landslides can be up to two orders of magnitude bigger than those that occur on land. Hazards related to such landslides, ranging from destruction of offshore facilities to collapse of coastal facilities and the generation of tsunamis, therefore occur widely.

Most submarine slopes are inherently stable and require external, often transient effects to trigger landslides. Elevated pore pressures, related to processes such as earthquake shaking or rapid sedimentation appear to be the critical factor in most submarine landslides. Such pore pressures support part or all of the weight of the overlying sediment, thus lowering the frictional resistance to landsliding. When concentrated in specific geological layers, they create weak layers, which fail in a characteristic bedding plane parallel style. The Storegga slide, off western Norway, is a classic example of this type of landslide showing several distinct gently sloping failure planes parallel to the sedimentary bedding, steep headwall scarps separating the different glide plane levels, retrogressive landslide behaviour, and clear evidence that most of the landslide mass deformed by brittle deformation.

Landslides on the flanks of oceanic volcanic islands, such as the Canary islands, have received much attention because of their potential tsunamigenic behaviour. While it is certain that such landslides have occurred in the past and will again occur in the future, the causes and triggers of flank failure are relatively poorly understood. The best evidence suggests that these landslides are retrogressive and occur over a period of hours or days, rather than the instantaneous failure of a single coherent block. It therefore seems unlikely that simple models that treat these landslides as single rapidly moving blocks can accurately predict their tsunamigenic potential. In any case, it needs to be remembered that any worst-case scenario model, such as that produced by Ward & Day (2001) for La Palma in the Canary islands, which maximizes every model parameter, has a low probability of occurrence in the real world.

The precise forecasting of submarine landslides is still largely beyond our ability—areas at risk from landslide are relatively easy to identify, but we are far from being able to forecast the occurrence of individual events. Numerical modelling of landslides and related hazards such as tsunamis is one of the most obvious ways in which our understanding can be improved. Such models can be used to help estimate the potential losses and risk to human life and infrastructure due to landslides that in turn can be used to construct mitigation strategies.

Petter Bryn of Norsk Hydro is thanked for providing the image of the Storegga slide used in figure 4. Michael Frenz kindly provided the grain size profiles and core images in figure 9. Dieter Issler and Farrokh Nadim contributed to the sections on landslide modelling and risk assessment, respectively. Funding provided by EU contracts EVK3-CT-2002-00079 (EUROSTRATAFORM) and HPRN-CT-2002-00212 (EURODOM) is gratefully acknowledged.

## References

- Assier-Rzadkiewicz, S., Heinrich, P., Sabatier, P. C., Savoye, B. & Bourillet, J. F. 2000 Numerical modelling of a landslide-generated tsunami: the 1979 Nice event. *Pure Appl. Geophys.* **157**, 1717–1727.
- Bardet, J.-P., Synolakis, C. E., Davies, H. L., Imamura, F. & Okal, E. A. 2003 Landslide tsunamis: recent findings and research directions. *Pure Appl. Geophys.* **160**, 1793–1809. (doi:10.1007/s00024-003-2406-0)
- Bentley, S. P. & Smalley, I. J. 1984 Landslips in sensitive clays. In *Slope instability* (ed. D. Brunsten & D. B. Prior), pp. 457–490. Chichester, UK: Wiley.
- Bondevik, S., Svendsen, J. I. & Mangerud, J. 1997 Tsunami sedimentary facies deposited by the Storegga tsunami in shallow marine basins and coastal lakes, western Norway. *Sedimentology* **44**, 1115–1131. (doi:10.1046/j.1365-3091.1997.d01-63.x)
- Bondevik, S., Lovholt, F., Harbitz, C. B., Mangerud, J., Dawson, A. G. & Svendsen, J. I. 2005 The Storegga slide tsunami—comparing field observations with numerical simulations. *Mar. Pet. Geol.* **22**, 195–208. (doi:10.1016/j.marpetgeo.2004.10.003)
- Bryn, P., Solheim, A., Berg, K., Lien, R., Forsberg, C. F., Hafidason, H., Ottesen, D. & Rise, L. 2003 The Storegga slide complex: repeated large scale landsliding in response to climatic cyclicity. In *Submarine mass movements and their consequences* (ed. J. Locat & J. Mienert), pp. 215–222. Dordrecht, Netherlands: Kluwer Academic Publishers.
- Bryn, P., Berg, K., Forsberg, C. F., Solheim, A. & Kvalstad, T. J. 2005 Explaining the Storegga slide. *Mar. Pet. Geol.* **22**, 11–19. (doi:10.1016/j.marpetgeo.2004.12.003)
- Bugge, T., Befring, S., Belderson, R. H., Eidvin, T., Jansen, E., Kenyon, N. H., Holtedahl, H. & Sejrup, H. P. 1987 A giant three-stage submarine slide off Norway. *Geo-Mar. Lett.* **7**, 191–198. (doi:10.1007/BF02242771)
- Bugge, T., Belderson, R. H. & Kenyon, N. H. 1988 The Storegga slide. *Phil. Trans. R. Soc. A* **325**, 357–388.
- Canals, M. *et al.* 2004 Slope failure dynamics and impacts from seafloor and shallow sub-seafloor geophysical data: case studies from the COSTA project. *Mar. Geol.* **213**, 9–72. (doi:10.1016/j.margeo.2004.10.001)
- Cantagrel, J. M., Arnaud, N. O., Ancochea, E., Fuster, J. M. & Huertas, M. J. 1999 Repeated debris avalanches on Tenerife and genesis of Las Canadas caldera wall (Canary islands). *Geology* **27**, 739–742. (doi:10.1130/0091-7613(1999)027<0739:RDAOTA>2.3.CO;2)
- Carracedo, J. C. 1996 A simple model for the genesis of large gravitational landslide hazards in the Canary islands. In *Volcano instability on the Earth and other planets* (ed. W. J. McGuire, A. P. Jones & J. Neuberg) *Geological Society London Special Publication*, vol. 110, pp. 125–135. London, UK: Geological Society.

- Dawson, A. G., Long, D. & Smith, D. E. 1988 The Storegga slides: evidence from eastern Scotland for a possible tsunami. *Mar. Geol.* **82**, 271–276. (doi:10.1016/0025-3227(88)90146-6)
- De Blasio, F., Elverhøi, A., Issler, D., Harbitz, C. B., Bryn, P. & Lien, R. 2005 On the dynamics of subaqueous clay rich gravity mass flows—the giant Storegga slide, Norway. *Mar. Pet. Geol.* **22**, 179–186. (doi:10.1016/j.marpetgeo.2004.10.014)
- Fine, I. V., Rabinovich, A. B., Bornhold, B. D., Thomson, R. E. & Kulikov, E. A. 2005 The Grand Banks landslide-generated tsunami of November 18, 1929: preliminary analysis and numerical modelling. *Mar. Geol.* **215**, 45–57. (doi:10.1016/j.margeo.2004.11.007)
- Forsberg, C. F. 2002 Reconstruction of the pre-Storegga slide stratigraphy. Norsk Hydro Report 37 00NH-X15-00040.
- Fryer, G. J., Watts, P. & Pratson, L. F. 2004 Source of the great tsunami of 1 April, 1946: a landslide in the upper Aleutian forearc. *Mar. Geol.* **203**, 201–218. (doi:10.1016/S0025-3227(03)00305-0)
- Garcia, M. O. 1996 Turbidites from slope failure on Hawaiian volcanoes. In *Volcano instability on the Earth and other planets* (ed. W. J. McGuire, A. P. Jones & J. Neuberg) *Geological Society London Special Publication*, vol. 110, pp. 281–294. London, UK: Geological Society.
- Gee, M. J. R., Masson, D. G., Watts, A. B. & Allen, P. A. 1999 The Saharan debris flow: an insight into the mechanics of long runout debris flows. *Sedimentology* **46**, 317–335. (doi:10.1046/j.1365-3091.1999.00215.x)
- Gee, M. J. R., Watts, A. B., Masson, D. G. & Mitchell, N. C. 2001 Landslides and the evolution of El Hierro in the Canary islands. *Mar. Geol.* **177**, 271–294. (doi:10.1016/S0025-3227(01)00153-0)
- Haffidason, H., Sejrup, H. P., Berstad, I. M., Nygard, A., Richter, T., Lien, R. & Berg, K. 2003 A weak layer feature on the northern Storegga slide escarpment. In *European margin sediment dynamics* (ed. J. Mienert & P. P. E. Weaver), pp. 55–62. Berlin, Germany: Springer.
- Haffidason, H., Sejrup, H. P., Nygard, A., Meinert, J., Bryn, P., Lien, R., Forsberg, C. F., Berg, K. & Masson, D. G. 2004 The Storegga slide: architecture, geometry and slide development. *Mar. Geol.* **213**, 201–234. (doi:10.1016/j.margeo.2004.10.007)
- Haffidason, H., Lien, R., Sejrup, H. P., Forsberg, C. F. & Bryn, P. 2005 The dating and morphometry of the Storegga slide. *Mar. Pet. Geol.* **22**, 123–136. Ormen Lange Special Issue. . (doi:10.1016/j.marpetgeo.2004.10.008)
- Hampton, M. A., Lee, H. J. & Locat, J. 1996 Submarine landslides. *Rev. Geophys.* **34**, 33–59. (doi:10.1029/95RG03287)
- Haugen, K. B., Lovholt, F. & Harbitz, C. B. 2005 Fundamental mechanisms for tsunami generation by submarine flows in idealised geometries. *Mar. Pet. Geol.* **22**, 209–217. (doi:10.1016/j.marpetgeo.2004.10.016)
- Heezen, B. C. & Ewing, M. 1952 Turbidity currents and submarine slumps, and the 1929 Grand Banks Earthquake. *Am. J. Sci.* **250**, 775–793.
- Hurlimann, M., Marti, J. & Ledesma, A. 2004 Morphological and geological aspects related to large slope failures on oceanic islands—the huge Orotava landslides on Tenerife, Canary islands. *Geomorphology* **62**, 143–158. (doi:10.1016/j.geomorph.2004.02.008)
- Hühnerbach, V., Masson, D. G. & COSTA project partners 2004 Landslides in the north Atlantic and its adjacent seas: an analysis of their morphology, setting and behaviour. *Mar. Geol.* **213**, 343–362. (doi:10.1016/j.margeo.2004.10.013)
- Hühnerbach, V., Masson, D. G., Bohrmann, G., Bull, J. M. & Weinrebe, W. 2005 Deformation and submarine landsliding caused by seamount subduction beneath the Costa Rican margin—new insights from high-resolution sidescan sonar data. In *Submarine slope systems: processes and products* (ed. D. M. Hodgson & S. S. Flint) *Geological Society Special Publication*, vol. 244, pp. 195–205. London, UK: Geological Society.
- Iltstad, T., Elverhøi, A., Issler, D. & Marr, J. G. 2004 Subaqueous debris flow behaviour and its dependence on the sand/clay ratio: a laboratory study using particle tracking. *Mar. Geol.* **213**, 415–418. (doi:10.1016/j.margeo.2004.10.017)
- Iverson, R. M. 1997 The physics of debris flows. *Rev. Geophys.* **35**, 245–296. (doi:10.1029/97RG00426)

- Jorstad, F. A. 1968 *Waves generated by landslides in Norwegian fjords and lakes*, vol. 79, pp. 13–31. Oslo, Norway: Norwegian Geotechnical Institute Publication.
- Kulikov, E. A., Rabinovich, A. B., Thomson, R. E. & Bornhold, B. D. 1996 The landslide tsunami of November 3, 1994 Skagway harbour, Alaska. *J. Geophys. Res.* **101**, 6609–6615. (doi:10.1029/95JC03562)
- Kvalstad, T. J., Andresen, L., Forsberg, C. F., Berg, K., Bryn, P. & Wangen, M. 2005 The Storegga slide: evaluation of triggering sources and slide mechanics. *Mar. Pet. Geol.* **22**, 245–256. (doi:10.1016/j.marpetgeo.2004.10.019)
- Laberg, J. S., Vorren, T. O., Mienert, J., Haflidason, H., Bryn, P. & Lien, R. 2003 Preconditions leading to the Holocene Traenadjupet slide, offshore Norway. In *Submarine mass movements and their consequences* (ed. J. Locat & J. Mienert), pp. 247–254. Dordrecht, Netherlands: Kluwer Academic Publishers.
- Lastras, G., Canals, M., Urgeles, R., Hughes-Clarke, J. E. & Acosta, J. 2004 Shallow slides and pockmark swarms in the Eivissa Channel, western Mediterranean sea. *Sedimentology* **51**, 1–14. (doi:10.1111/j.1365-3091.2004.00654.x)
- Lay, T. *et al.* 2005 The great Sumatra–Andaman earthquake of 26 December, 2004. *Science* **308**, 1127–1133. (doi:10.1126/science.1112250)
- Locat, J., Martin, F., Levesque, C., Locat, P., Leroueil, S., Konrad, J.-M., Urgeles, R., Canals, M. & Duchesne, M. J. 2003 Submarine mass movements in the upper Saguenay Fjord (Quebec, Canada) triggered by an earthquake. In *Submarine mass movements and their consequences* (ed. J. Locat & J. Mienert), pp. 509–519. Dordrecht, Netherlands: Kluwer Academic Publishers.
- Longva, O., Janbu, N., Blikra, L. H. & Boe, R. 2003 The Finneidfjord slide: seafloor failure and slide dynamics. In *Submarine mass movements and their consequences* (ed. J. Locat & J. Mienert), pp. 531–538. Dordrecht, Netherlands: Kluwer Academic Publishers.
- Lovholt, F., Harbitz, C. B. & Haugen, K. B. 2005 A parametric study of tsunamis generated by submarine slides in the Ormen Lange/Storegga area off western Norway. *Mar. Pet. Geol.* **22**, 219–231. (doi:10.1016/j.marpetgeo.2004.10.017)
- Lynett, P. J., Borrero, J. C., Liu, P. L.-F. & Synolakis, C. E. 2003 Field survey and numerical simulations: a review of the 1998 Papua New Guinea tsunami. *Pure Appl. Geophys.* **160**, 2119–2146. (doi:10.1007/s00024-003-2422-0)
- Mader, C. L. 2001 Modelling the La Palma landslide tsunami. *Sci. Tsunami Hazards* **19**, 150–170.
- Masson, D. G. 1996 Catastrophic collapse of the flank of El Hierro about 15,000 years ago, and the history of large flank collapses in the Canary islands. *Geology* **24**, 231–234. (doi:10.1130/0091-7613(1996)024<0231:CCOTVI>2.3.CO;2)
- Masson, D. G. 2001 Sedimentary processes shaping the eastern slope of the Faeroe-Shetland channel. *Continental Shelf Res.* **21**, 825–857. (doi:10.1016/S0278-4343(00)00115-1)
- Masson, D. G., Canals, M., Alonso, B., Urgeles, R. & Hühnerbach, V. 1998 The Canary Debris flow: source area morphology and failure mechanisms. *Sedimentology* **45**, 411–432. (doi:10.1046/j.1365-3091.1998.0165f.x)
- Masson, D. G., Watts, A. B., Gee, M. R. J., Urgeles, R., Mitchell, N. C., Le Bas, T. P. & Canals, M. 2002 Slope failures on the flanks of the western Canary islands. *Earth Sci. Rev.* **57**, 1–35. (doi:10.1016/S0012-8252(01)00069-1)
- Matsumoto, T. & Tappin, D. R. 2003 Possible coseismic large-scale landslide off the northern coast of Papua New Guinea in July 1998: geophysical and geological results of the SOS cruises. *Pure Appl. Geophys.* **160**, 1923–1943. (doi:10.1007/s00024-003-2414-0)
- McMurty, G. M., Watts, P., Fryer, G. J., Smith, J. R. & Inamura, F. 2004 Giant landslides, mega-tsunamis and paleo-sealevel in the Hawaiian islands. *Mar. Geol.* **203**, 219–234. (doi:10.1016/S0025-3227(03)00306-2)
- McSaveney, M. J., Goff, J. R., Darby, D. J., Goldsmith, P., Barnett, A., Elliot, S. & Nongkas, M. 2000 The 17 July 1998 tsunami, Papua New Guinea: evidence and initial interpretation. *Mar. Geol.* **170**, 81–92. (doi:10.1016/S0025-3227(00)00067-0)

- Moore, J. G., Clague, D. A., Holcomb, R. T., Lipman, P. W., Normark, W. R. & Torresan, M. E. 1989 Prodigious submarine landslides on the Hawaiian Ridge. *J. Geophys. Res.* **94**, 17 465–17 484.
- Moore, J. G., Normark, W. R. & Holcomb, R. T. 1994 Giant Hawaiian landslides. *Ann. Rev. Earth Planet. Sci.* **22**, 119–144. (doi:10.1146/annurev.earth.22.050194.001003)
- Mulder, T. & Alexander, J. 2001 The physical character of subaqueous sedimentary debris flows and their deposits. *Sedimentology* **48**, 269–299. (doi:10.1046/j.1365-3091.2001.00360.x)
- Mulder, T. & Cochonot, P. 1996 Classification of offshore mass movements. *J. Sed. Res.* **66**, 43–57.
- O’Leary, D. W. 1991 Structure and morphology of submarine slab slides: clues to origin and behaviour. *Mar. Geotech.* **10**, 53–69.
- Okal, E. A. & Synolakis, C. E. 2004 Source discriminants for near-field tsunamis. *Geophys. J. Int.* **158**, 899–912. (doi:10.1111/j.1365-246X.2004.02347.x)
- Ollier, G., Cochonot, P., Lenat, J. F. & Labazuy, P. 1998 Deep-sea volcanoclastic sedimentary systems: an example from La Fournaise volcano, Reunion island, Indian Ocean. *Sedimentology* **45**, 293–330. (doi:10.1046/j.1365-3091.1998.0152e.x)
- Pearce, T. J. & Jarvis, I. 1992 Applications of geochemical data to modelling sediment dispersal patterns in distal turbidites: late Quaternary of the Madeira Abyssal Plain. *J. Sed. Petrol.* **62**, 1112–1129.
- Piper, D. J. W., Cochonot, P. & Morrison, M. L. 1999 The sequence of events around the epicentre of the 1929 Grand Banks earthquake: initiation of debris flows and turbidity currents inferred from sidescan sonar. *Sedimentology* **46**, 79–97. (doi:10.1046/j.1365-3091.1999.00204.x)
- Plafker, G. & Ericksen, G. E. 1978 Nevados Huascarán avalanche, Peru. In *Rockslides and avalanches, 1. Natural phenomena* (ed. B. Voight), pp. 277–314. Amsterdam, Netherlands: Elsevier Scientific Publishing Company.
- Prior, D. B. & Coleman, J. M. 1982 Active slides and flows in underconsolidated marine sediments on the slope of the Mississippi delta. In *Marine slides and other mass movements* (ed. S. Saxov & J. K. Nieuwenhuis), pp. 21–49. New York, NY: Plenum Press.
- Prior, D. B., Bornhold, B. D., Coleman, J. M. & Bryant, W. R. 1982 Morphology of a submarine slide, Kitimat Arm, British Columbia. *Geology* **10**, 588–592. (doi:10.1130/0091-7613(1982)10<588:MOASSK>2.0.CO;2)
- Roberts, J. A. & Cramp, A. 1996 Sediment stability on the western flanks of the Canary islands. *Mar. Geol.* **134**, 13–30. (doi:10.1016/0025-3227(96)00021-7)
- Rothwell, R. G., Pearce, T. J. & Weaver, P. P. E. 1992 Late quaternary evolution of the Madeira Abyssal plain, NE Atlantic. *Basin Res.* **4**, 103–131.
- Satake, K. & Tanioka, Y. 2003 The July 1998 Papua New Guinea Earthquake: mechanism and quantification of unusual tsunami generation. *Pure Appl. Geophys.* **160**, 2087–2188. (doi:10.1007/s00024-003-2421-1)
- Solheim, A., Berg, K., Forsberg, C. F. & Bryn, P. 2005 The Storega slide complex: repetitive large scale sliding with similar cause and development. *Mar. Petrol. Geol.* **22**, 97–107. (doi:10.1016/j.marpetgeo.2004.10.013)
- Sultan, N., Cochonot, P., Foucher, J. P., Mienert, J., Haffidason, H. & Sejrup, H. P. 2003 Effect of gas hydrates dissociation on seafloor slope stability. In *Submarine mass movements and their consequences* (ed. J. Locat & J. Mienert), pp. 103–111. Dordrecht, Netherlands: Kluwer Academic Publishers.
- Sweet, S. & Silver, E. A. 2003 Tectonics and slumping in the source region of the 1998 Papua New Guinea tsunami from seismic reflection images. *Pure Appl. Geophys.* **160**, 1945–1968. (doi:10.1007/s00024-003-2415-z)
- Talling, P. J. *et al.* 2002 Experimental constraints on shear mixing rates and processes: implications for the dilution of submarine debris flows. In *Glacier-influenced sedimentation on high-latitude continental margins* (ed. J. A. Dowdeswell & C. O’Cofaigh) *Geological Society Special Publication*, vol. 203, pp. 89–104. London, UK: Geological Society.
- Tappin, D. R., Watts, P., McMurty, G. M., Lafoy, Y. & Matsumoto, T. 2001 The Sissano, Papua New Guinea tsunami of July, 1998—offshore evidence on the source mechanism. *Mar. Geol.* **175**, 1–24. (doi:10.1016/S0025-3227(01)00131-1)

- Urgeles, R., Canals, M., Baraza, J., Alonso, B. & Masson, D. G. 1997 The most recent megaslides on the Canary islands: the El Golfo Debris avalanche and the Canary Debris flow. *J. Geophys. Res.* **102**, 20 305–20 323. see also 323. (doi:10.1029/97JB00649)
- Voight, B. & Pariseau, W. G. 1978 Rockslides and avalanches: an introduction. In *Rockslides and avalanches, 1. Natural phenomena* (ed. B. Voight), pp. 1–67. Amsterdam, Netherlands: Elsevier Scientific Publishing Company.
- Ward, S. N. 2001 Landslide tsunami. *J. Geophys. Res.* **106**, 11 201–11 215. (doi:10.1029/2000JB900450)
- Ward, S. N. & Day, S. J. 2001 Cumbre Vieja volcano—potential collapse and tsunami at La Palma, Canary islands. *Geophys. Res. Lett.* **28**, 3397–3400. (doi:10.1029/2001GL013110)
- Ward, S. N. & Day, S. J. 2003 Ritter island volcano—lateral collapse and the tsunami of 1888. *Geophys. J. Int.* **154**, 891–902. (doi:10.1046/j.1365-246X.2003.02016.x)
- Watts, A. B. & Masson, D. G. 1995 A giant landslide on the north flank of Tenerife, Canary islands. *J. Geophys. Res.* **100**, 24 487–24 498. (doi:10.1029/95JB02630)
- Watts, A. B. & Masson, D. G. 2001 New sonar evidence for recent catastrophic collapses of the north flank of Tenerife, Canary islands. *Bull. Volcanol.* **63**, 8–19. (doi:10.1007/s004450000119)
- Weaver, P. P. E. & Kuijpers, A. 1983 Climatic control of turbidite deposition on the Madeira Abyssal plain. *Nature* **306**, 360–363. (doi:10.1038/306360a0)
- Weaver, P. P. E., Wynn, R. B., Kenyon, N. H. & Evans, J. 2000 Continental margin sedimentation with special reference to the Northeast Atlantic margin. *Sedimentology* **47**, 239–256. (doi:10.1046/j.1365-3091.2000.0470s1239.x)
- Wilson, C. K., Long, D. & Bulat, J. 2004 The morphology, setting and processes of the Afen slide. *Mar. Geol.* **213**, 149–167. (doi:10.1016/j.margeo.2004.10.005)
- Wynn, R. B. & Masson, D. G. 2003 Canary island landslides and tsunami generation: can we use turbidite deposits to interpret landslide processes. In *Submarine mass movements and their consequences* (ed. J. Locat & J. Mienert), pp. 325–332. Dordrecht, Netherlands: Kluwer Academic Publishers.
- Wynn, R. B., Weaver, P. P. E., Stow, D. A. V. & Masson, D. G. 2002 Turbidite depositional architecture across three interconnected deep-water basins on the northwest African margin. *Sedimentology* **49**, 1441–1462. (doi:10.1046/j.1365-3091.2002.00471.x)